OPEN

Journal of Human Genetics (2014) 59, 129–133

www.nature.com/jhg

ORIGINAL ARTICLE

Clinical and genetic analysis of the first known Asian family with myotonic dystrophy type 2

Takahiro Nakayama[1], Harumasa Nakamura[2], Yasushi Oya[2], Takashi Kimura[3], Ichiro Imahuku[1], Kinji Ohno[4], Ichizo Nishino[5], Koji Abe[6] and Tohru Matsuura[6,7]

Myotonic dystrophy type 2 (DM2) is more common than DM1 in Europe and is considered a rare cause of myotonic dystrophies in Asia. Its clinical course is also milder with more phenotypic variability than DM1. We herein describe the first known Asian family (three affected siblings) with DM2 based on clinical and genetic analyses. Notably, two of the affected siblings were previously diagnosed with limb-girdle muscular dystrophy. Myotonia (the inability of the muscle to relax) was absent or only faintly present in these individuals. The third sibling had grip myotonia and is the first known Asian DM2 patient. The three DM2 siblings share several systemic characteristics, including late-onset, proximal-dominant muscle weakness, diabetes, cataracts and asthma. Repeat-primed PCR across the DM2 repeat revealed a characteristic ladder pattern of a CCTG expansion in all siblings. Southern blotting analysis identified the presence of 3400 repeats. Further DM2 studies in Asian populations are needed to define the clinical presentation of Asian DM2 and as yet unidentified phenotypic differences from Caucasian patients.
Journal of Human Genetics (2014) **59**, 129–133; doi:10.1038/jhg.2013.133; published online 16 January 2014

Keywords: Asian; CCTG repeat; clinical spectrum; haplotype; limb-girdle muscular dystrophy; myotonia; myotonic dystrophy type 2 (DM2)

INTRODUCTION

Myotonic dystrophy (DM) is the most common adult-onset muscular dystrophy and is characterized by autosomal dominant progressive myopathy (muscle weakness), myotonia (the inability of the muscle to relax) and multiorgan involvement. Two genetically distinct forms of the disease with clinical similarities but distinct differences are known: DM type 1 (DM1) and type 2 (DM2). DM1 is caused by the expansion of a CTG repeat in the 3′-untranslated region of the dystrophia myotonica-protein kinase gene on chromosome 19p13.3,[1] while DM2 is caused by an expansion of a tetranucleotide CCTG repeat in the first intron of the cellular nucleic acid-binding protein (*CNBP*, formerly *ZNF9*) gene on chromosome 3q21.[2] The unprecedented number of expanded DM2 CCTG repeats (ranging from 75 to 11 000 with a mean of 5000) is highly unstable in intergenerational transmissions and varies in a tissue-specific, time-dependent manner.[2]

The clinical severity and spectrum of DM2 is highly variable, and this is not thought to be associated with the length of repeat expansions.[2,3] Most DM2 mutations have been identified in European Caucasians that originate from a single common founder and share an identical haplotype.[4–6] However, we previously identified the first Japanese DM2 patient carrying a haplotype distinct from that shared among Caucasians, indicating that DM2 exists in non-Caucasian populations and has separate founders.[7] Thus, it would be beneficial to investigate whether DM2 patients of different ethnicities and haplotypes have a comparable phenotype to the predominantly European patients with a common haplotype. To further characterize the variable clinical phenotype of DM2, we describe the clinical and molecular findings of the first known Asian family with DM2, including the previously reported Japanese female patient[7] and her two affected siblings.

SUBJECTS AND METHODS

The pedigree studied is shown in Figure 1. DNA was extracted from peripheral blood samples obtained from the three affected family members with their informed consent. Approval for the study was obtained from the ethics committees of Okayama University, Nagoya University Graduate School of Medicine and the National Center of Neurology and Psychiatry.

PCR products across the DM2 repeat (marker CL3N58)[2] in the first intron of *CNBP* were analyzed by capillary electrophoresis using an automated DNA sequencer (ABI 310A Genetic Analyzer, Applied Biosystems, Foster City, CA, USA). The PCR reaction was performed in a 20 μl volume containing 100 ng genomic DNA as template, 1 × HotStarTaq *Plus* Master Mix (Qiagen, Valencia, CA, USA) and 0.2 μM each of the primers: 6FAM-fluorescent-labeled

[1]Department of Neurology, Yokohama Rosai Hospital, Yokohama, Japan; [2]Department of Neurology, National Center Hospital, National Center of Neurology and Psychiatry, Tokyo, Japan; [3]Department of Neurology, Asahikawa Medical Center, National Hospital Organization, Asahikawa, Japan; [4]Division of Neurogenetics, Center for Neurological Diseases and Cancer, Nagoya University Graduate School of Medicine, Nagoya, Japan; [5]Department of Neuromuscular Research, National Institute of Neuroscience, National Center of Neurology and Psychiatry, Tokyo, Japan; [6]Department of Neurology, Okayama University Graduate School of Medicine, Dentistry and Pharmaceutical Sciences, Okayama, Japan and [7]Division of Neurology, Department of Medicine, Jichi Medical University, Shimotsuke, Japan
Correspondence: Dr T Matsuura, Division of Neurology, Department of Medicine, Jichi Medical University, 3311-1 Yakushiji, Shimotsuke, Tochigi 329-0498, Japan. E-mail:tohrum@jichi.ac.jp
Received 20 March 2013; revised 16 November 2013; accepted 4 December 2013; published online 16 January 2014

CL3N58-D F (5′-GCCTAGGGGACAAAGTGAGA-3′) and CL3N58-D R (5′-GGCCTTATAACCATGCAAATG-3′). The PCR conditions consisted of an initial denaturation at 95 °C for 5 min, then 30 cycles of 94 °C for 30 s, 57 °C for 30 s and 72 °C for 30 s, with an additional extension at 72 °C for 10 min.

To detect the DM2 CCTG expansion, the repeat-primed PCR assay using an oligonucleotide primed within the DM2 CCTG repeat and Southern blotting analysis were performed as described elsewhere.[2,3,7,8] Briefly, repeat-primed PCR[8] was performed in a 20 µl volume containing 100 ng genomic DNA as template, 1 × HotStarTaq *Plus* Master Mix (Qiagen), 1 M betaine, 0.2 µM 6FAM-fluorescent-labeled CL3N58-D F (5′-GCCTAGGGGACAAAGTG AGA-3′), 0.05 µM reverse primer consisting of five CCTG repeats with an anchor tail: DM2-CCTG-for (5′-AGCGGATAACAATTTCACACAGGACCTGC CTGCCTGCCTGCCTG-3′) and 0.3 µM anchor primer corresponding to the anchor tail of the reverse primer: P3 (5′-AGCGGATAACAATTTCACACA GGA-3′). The PCR conditions were as follows: initial denaturation at 95 °C for 5 min, then 35 cycles of 94 °C for 1 min, 61 °C for 1 min and 72 °C for 1 min, with an additional extension at 72 °C for 10 min. Fragment length analysis was performed on an ABI 310A Genetic Analyzer. Southern blotting was carried out with *Eco*RI-digested DNA (10 µg) separated on an 0.8% agarose gel, which was transferred to a positively charged nylon membranes (Roche, Indianapolis, IN, USA) and hybridized with a 474-bp *CNBP* probe.[2]

RESULTS

Genetic studies

Three patients with DM2 CCTG expansion were identified in this pedigree. Case 3 has been reported previously.[7] All cases showed one peak following PCR of the DM2 repeat and a characteristic ladder pattern by repeat-primed PCR,[3,7] confirming the presence of the CCTG expansion (Figure 2). DNA extracted from the Case 2 individual was degraded, so Southern blotting hybridization analysis was performed on the remaining two patients (Cases 1 and 3). This showed the presence of an 18.1 kb expanded DM2 allele, corresponding to 3400 CCTG repeats (Figure 3).

Case reports

Table 1 summarizes the clinical manifestations of three symptomatic siblings carrying the DM2 mutation. The siblings share common clinical features, including adult-onset proximal dominant progressive weakness, cataracts, diabetes, cardiac arrhythmias and hypercholesteremia, as described in the previous literature on DM2.[7] The degree of myotonia (the cardinal feature of DM) is variable, with two siblings having little or no myotonia. Interestingly, all three were asthmatic. The data of allergic and autoimmune tests are shown in Table 2. The other asymptomatic members of the pedigree were not assessed.

Case 1

A 69-year-old Japanese woman first presented at the age of 64 years with a slowly progressive difficulty in walking. Her calves had become

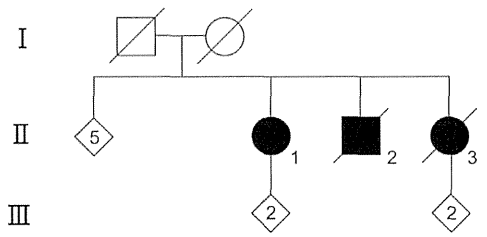

Figure 1 Pedigree of the sibling cases carrying the DM2 expansion. The parents did not suffer from muscle weakness and died at the ages of 67 and 72 years. The gender of the unaffected siblings and children of the affected cases is obscured to protect privacy.

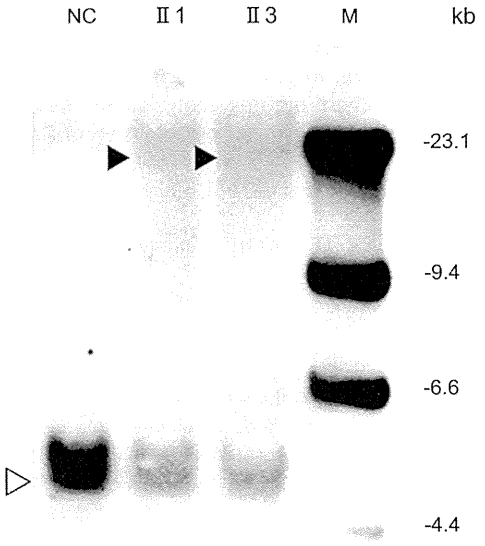

Figure 3 Southern blotting analysis of DM2. Closed arrowhead shows the expanded alleles in DM2. M, λDNA/*Hind* III marker; NC, normal control; II1 and II3, Cases 1 and 3 showing an 18.1-kb expanded allele as well as a normal allele (open arrowhead).

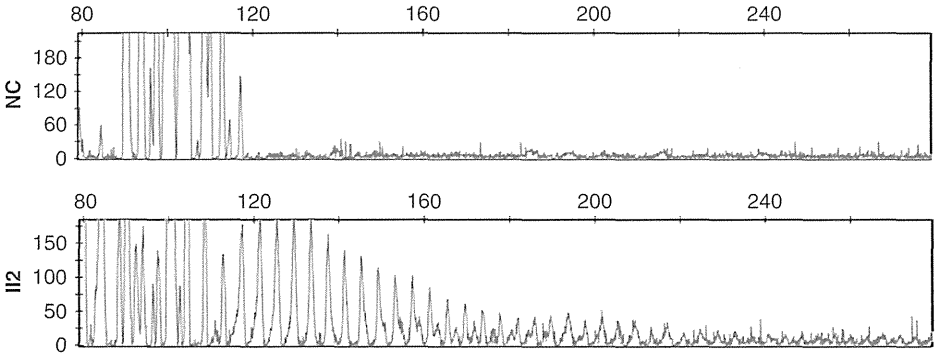

Figure 2 Repeat-primed PCR analysis specific for the DM2 expansion. Negative results from normal control (NC) are shown in the upper panel, whereas a characteristic continuous ladder from Case 2 (II2 in Figure 1), indicating the CCTG expansion, is detected in the lower panel. A full color version of this figure is available at the *Journal of Human Genetics* journal online.

Table 1 Clinical features of DM2 patients in the Japanese pedigree

	DM2 individuals		
Characteristic	*Case 1*	*Case 2*	*Case 3*[7]
Age (years)/gender	69/F	61/M	59/F
Age at DM2 onset (years)	64	50	47
Skeletal muscle features			
Myotonia			
Grip/percussion	−/+	−/−	+/+
EMG diagnosis	−/+	−	+
Myalgia/stiffness	+	−/−	−/−
Muscle weakness/atrophy			
Facial muscles	+	−	+
Sternocleidomastoids	+	+	+
Limbs	Proximal dominant	Proximal dominant	Proximal dominant
Systemic features			
Cataracts, by history of extraction (age in years)	59	62	52
Diabetes, by history (age in years)	33	40	47
ECG	Normal	Normal	cRBBB
Holter monitoring	PVC	PVC	PVC
Other disorders	Asthma, HT, low IgG Hypercholesterolemia Hyperthyroidism	Asthma, HT Hypercholesterolemia	Asthma, low IgG Hypercholesterolemia
Initial clinical diagnosis	LGMD	LGMD	Myotonic dystrophy

Abbreviations: cRBBB, complete right bundle branch block; DM2, myotonic dystrophy type 2; EMG, electromyogram; ECG, electrocardiogram; F, female; HT, hypertension; IgG, immunoglobulin G; LGMD, limb-girdle muscular dystrophy; M, male; PVC, premature ventricular contraction.

Table 2 Profile of autoantibodies, IgE and eosinophils in this pedigree

	DM2 individuals		
	Case 1	*Case 2*	*Case 3*[7]
Antinuclear antiboby	Negative	Negative	Negative
Rheumatoid factor	Negative	Negative	Negative
Anti-thyroglobulin antibody	Positive	NE	Negative
TSH receptor antibody	Positive	NE	Negative
IgE (normal: $<250\,IU\,ml^{-1}$)	NE	1700	52.8
Eosinophils (normal: 0–5% of leukocytes)	0–25	10.4–13.9	3

Abbreviations: DM2, myotonic dystrophy type 2; IgE, immunoglobulin E; NE, not examined; TSH, thyroid stimulating hormone.

stiff over the last 2 or 3 years. There was no history of developmental milestone delay. She had a past medical history of taking asthma and hyperthyroidism medication. At 33 years of age, she had developed type 2 diabetes mellitus and hypertension. At 59 years, she had had both posterior subcapsular cataracts extracted. There was no complaint of myalgia. There was no known consanguinity or genetic admixture with other ethnicities in her family, as described elsewhere.[7] Neither of her parents, her three older brothers, two older sisters nor either of her two children had been referred with evident muscle symptoms. On examination, she was able to walk upstairs by holding onto a rail and walking on flat ground. She showed mild facial weakness as well as weakness and atrophy of sternocleidomastoid muscles. Motor examination showed slight symmetric muscle atrophy and predominant proximal weakness. Percussion myotonia could be slightly induced in the tongue and thenar eminence; however, grip myotonia was not present. Tendon reflexes were within the normal range. There were no cerebellar, sensory or autonomic disorders. Serum creatine kinase elevation was evident at $413\,IU\,l^{-1}$ (normal range: $37–115\,IU\,l^{-1}$), and high hemoglobin A1c (7.6%) and total cholesterol levels ($248\,mg\,dl^{-1}$) were seen. The serum immunoglobulin G level was slightly decreased to $808\,mg\,dl^{-1}$ (normal range: $870–1700\,mg\,dl^{-1}$). Holter monitoring detected premature ventricular contractions. Electromyography showed small motor unit potentials with occasional myotonic discharges in all the muscles examined. Nerve conduction studies were normal. Muscle computed tomography revealed diffuse muscle atrophy in the trunk and proximally in all limbs, whereas forearm and distal leg muscles were well preserved. Fluid-attenuated inversion recovery and T2-weighted brain magnetic resonance imaging showed non-specific periventricular white matter hyperintensities without significant cerebral atrophy.

Case 2

A 61-year-old man, the younger brother of case 1, began to notice difficulty lifting his knees when climbing mountains or stairs at the age of 50 years. He had had a normal birth and development. At the age of 55 years, he had started to hold onto something when rising from a supine or sitting position and to feel difficulty in lifting his right arm. At 40 years of age, he had developed type 2 diabetes mellitus and hypertension. At 62 years, he had a left posterior subcapsular cataract extracted. He had a past medical history of taking asthma medication. He was referred to our hospital by his primary physician because of an elevated creatine kinase level of

1094 IU l^{-1} (normal range: <195 IU l^{-1}). There was no complaint of muscle pain or stiffness.

Neurologically, the patient had normal language, speech and cognition on routine clinical evaluation. There were no cranial nerve abnormalities except for mild atrophy and weakness of the bilateral sternocleidomastoid muscles. Motor examination revealed predominant proximal muscle weakness and atrophy in all the limbs. In particular, atrophy of the right deltoid muscle and infraspinatus muscle and weakness of the right shoulder abduction and extortion were remarkable. There was no grip or percussion myotonia. Tendon reflexes were present but were hypoactive in both upper limbs. There were no cerebellar, sensory or autonomic disorders. There was slight serum creatine kinase elevation at 321 IU l^{-1} (normal range: 62–287 IU l^{-1}) and high hemoglobin A1c (7.2%) and total cholesterol levels (271 mg dl^{-1}). The serum immunoglobulin G level was 915 mg dl^{-1} (normal range: 870–1700 mg dl^{-1}). The electrocardiogram was normal, but 24-h Holter monitoring detected occasional premature ventricular contractions. Electromyography showed small motor unit potentials with early recruitment and complex repetitive discharges in all the muscles examined. No myotonic discharges were observed. Nerve conduction studies were normal. Muscle computed tomography revealed diffuse muscle atrophy in the trunk and proximally in all the limbs, whereas forearm and distal leg muscles were well preserved. The patient died from gastric cancer at the age of 66 years. Brain magnetic resonance imaging at the age of 65 years was normal without significant cerebral atrophy.

Case 3

The clinical presentation of Case 3 was previously described by Saito *et al.*[7] In addition, the patient had a past medical history of bronchial asthma, and hypercholesterolemia was detected (282 mg dl^{-1}) at the age of 59 years. The patient died suddenly at the age of 66 years of unknown causes.

DISCUSSION

This is the first known report of an Asian family with DM2. As expected for a dominantly inherited disorder, approximately 50% of first-degree relatives are at risk for DM2. However, given that clinical information is only available for three affected individuals among 13 members of a family of three consecutive generations, incomplete penetrance with asymptomatic carriers is the more favorable explanation of the pedigree. It could also reflect insufficient information about mild symptoms or signs in the past.

Notably, two of the affected members (Cases 1 and 2) had previously been diagnosed with limb-girdle muscular dystrophy because of the absence or subtlety of myotonia until their younger sister (Case 3) was genetically confirmed as the first Asian DM2 patient. Based on a report by Day *et al.*,[3] 90% of affected DM2 individuals from the European and American families have electrical myotonia and 75% have clinical myotonia. There is a possibility that Japanese/Asian DM2 individuals are underdiagnosed or misdiagnosed as another muscle disease because of the lack of myotonia[9] and the previous conception of the rarity of DM2 in Asian populations.[10] As seen in other repeat expansion disorders such as spinocerebellar ataxia type 2 (SCA2), Machado–Joseph disease/SCA3 and SCA10,[11–13] we also have to keep in mind the clinical differences between different ethnicities and geographical regions, which cannot be explained by the repeat size. A unique Japanese/Asian haplotype mutation[7] may also be related to low disease penetrance or the clinical presentation of mild DM2.

Multi-systemic features such as cataracts, diabetes, obesity, hypogammaglobulinemia, cardiac conduction block and arrhythmia are often seen in both DM1 and DM2 patients.[3,14] In addition, a strong association between Dutch DM2 patients and autoimmune diseases or autoantibody production was recently reported, in contrast with those with DM1 whose data were comparable with the general population.[15] Interestingly, all three patients in the present study were asthmatic, yet this association has not been previously described in the literature. To examine whether it is a true association or a mere coincidence, more families with different genetic backgrounds should be investigated. It is conceivable that the DM2 expansion directly affects the immune system or that the co-existence of a genetic change in flanking regions in linkage disequilibrium with the DM2 expansion confers susceptibility to allergic or autoimmune diseases.

It is well known that non-coding repeat expansion disorders, especially DM2, are associated with intra/inter-familial clinical variations and complex genotype–phenotype correlations.[2,3] Therefore, to achieve an improved diagnosis of DM2, clinicians should examine as many family members as possible in the same pedigree and be aware of its wide clinical spectrum, which is possibly influenced by racial and environmental factors. Although this study could not determine characteristic features in Asian DM2, further collection of additional Asian DM2 families is needed to investigate clinical and genetic differences between Caucasian and Asian patients with DM2. Comparison of the association between phenotype and ethnic/haplotype differences will be made possible in the future by the clinical and genetic assessment of DM2 subjects with different founders.

CONFLICT OF INTEREST

The authors declare no conflicts of interest.

ACKNOWLEDGEMENTS

We are grateful to the patients and their family for participating in this study. The study was supported by JSPS KAKENHI Grant Numbers 24390083, 23659455 (to TM), 20390250 (to IN), 21390267 (to KA) and 24390221 (to KO), as well as Research Grants (to TM, IN, KA and KO) for Intractable Diseases from the Ministry of Health, Labour and Welfare of Japan.

1 Harper, P. S. in *Myotonic Dystrophy* (W.B. Saunders, London, UK, 2001).
2 Liquori, C. L., Ricker, K., Moseley, M. L., Jacobsen, J. F., Kress, W., Naylor, S. L. *et al.* Myotonic dystrophy type 2 caused by a CCTG expansion in intron 1 of ZNF9. *Science* **293,** 864–867 (2001).
3 Day, J. W., Ricker, K., Jacobsen, J. F., Rasmussen, L. J., Dick, K. A., Kress, W. *et al.* Myotonic dystrophy type 2: molecular, diagnostic and clinical spectrum. *Neurology* **60,** 657–664 (2003).
4 Liquori, C. L., Ikeda, Y., Weatherspoon, M., Ricker, K., Schoser, B. G., Dalton, J. C. *et al.* Myotonic dystrophy type 2: human founder haplotype and evolutionary conservation of the repeat tract. *Am. J. Hum. Genet.* **73,** 849–862 (2003).
5 Bachinski, L. L., Udd, B., Meola, G., Sansone, V., Bassez, G., Eymard, B. *et al.* Confirmation of the type 2 myotonic dystrophy $(CCTG)_n$ expansion mutation in patients with proximal myotonic myopathy/proximal myotonic dystrophy of different European origins: a single shared haplotype indicates an ancestral founder effect. *Am. J. Hum. Genet* **73,** 835–848 (2003).
6 Coenen, M. J., Tieleman, A. A., Schijvenaars, M. M., Leferink, M., Ranum, L. P., Scheffer, H. *et al.* Dutch myotonic dystrophy type 2 patients and a North-African DM2 family carry the common European founder haplotype. *Eur. J. Hum. Genet.* **19,** 567–570 (2011).
7 Saito, T., Amakusa, Y., Kimura, T., Yahara, O., Aizawa, H., Ikeda, Y. *et al.* Myotonic dystrophy type 2 in Japan: ancestral origin distinct from Caucasian families. *Neurogenetics* **9,** 61–63 (2008).

8 Radvansky, J., Ficek, A. & Kadasi, L. Upgrading molecular diagnostics of myotonic dystrophies: multiplexing for simultaneous characterization of the *DMPK* and *ZNF9* repeat motifs. *Mol. Cell Probes* **25,** 182–185 (2011).
9 Young, N. P., Daube, J. R., Sorenson, E. J. & Milone, M. Absent, unrecognized, and minimal myotonic discharges in myotonic dystrophy type 2. *Muscle Nerve* **41,** 758–762 (2010).
10 Matsuura, T., Minami, N., Arahata, H., Ohno, K., Abe, K., Hayashi, Y. K. *et al.* Myotonic dystrophy type 2 is rare in the Japanese population. *J. Hum. Genet.* **57,** 219–220 (2012).
11 Gwinn-Hardy, K., Chen, J. Y., Liu, H. C., Liu, T. Y., Boss, M., Seltzer, W. *et al.* Spinocerebellar ataxia type 2 with parkinsonism in ethnic Chinese. *Neurology* **55,** 800–805 (2000).
12 Subramony, S. H., Hernande,z, D., Adam, A., Smith-Jefferson, S., Hussey, J., Gwinn-Hardy, K. *et al.* Ethnic differences in the expression of neurodegenerative disease: Machado–Joseph disease in Africans and Caucasians. *Mov. Disord.* **17,** 1068–1071 (2002).
13 Teive, H. A., Roa, B. B., Raskin, S., Fang, P., Arruda, W. O., Neto, Y. C. *et al.* Clinical phenotype of Brazilian families with spinocerebellar ataxia 10. *Neurology* **63,** 1509–1512 (2004).
14 Meola, G. & Moxley, R. T. III Myotonic dystrophy type 2 and related myotonic disorders. *J. Neurol.* **252,** 1173–1182 (2004).
15 Tieleman, A. A., den Broeder, A. A., van de Logt, A. E. & van Engelen, B. G. Strong association between myotonic dystrophy type 2 and autoimmune diseases. *J. Neurol. Neurosurg. Psychiatry* **80,** 1293–1295 (2009).

Journal of Clinical Neuroscience 21 (2014) 1341–1343

Contents lists available at ScienceDirect

Journal of Clinical Neuroscience

journal homepage: www.elsevier.com/locate/jocn

Clinical Study

Seven amyotrophic lateral sclerosis patients diagnosed only after development of respiratory failure

Kota Sato, Nobutoshi Morimoto, Kentaro Deguchi, Yoshio Ikeda, Tohru Matsuura, Koji Abe *

Department of Neurology, Okayama University Graduate School of Medicine, Dentistry and Pharmaceutical Sciences, and Okayama University Hospital, 2-5-1 Shikata-cho, Kita-ku, Okayama 700-8558, Japan

ARTICLE INFO

Article history:
Received 18 September 2012
Accepted 10 November 2013

Keywords:
ALS
Emergency medicine
Intubation
Neurodegenerative disorder
Respiratory failure

ABSTRACT

Amyotrophic lateral sclerosis (ALS) is a progressive, neurodegenerative disorder that causes muscle weakness, disability, respiratory failure, and eventually death. However, some ALS patients are diagnosed only after development of respiratory failure. To study the reason for delayed diagnosis of ALS, we reviewed cases of ALS patients with respiratory failure. We retrospectively reviewed all 200 patients diagnosed with sporadic ALS in our hospital from January 2001 to April 2011. Among them, we focused on seven patients who were diagnosed only after developing respiratory failure. We reviewed their clinical characteristics and demographics. The mean time from onset to a correct diagnosis was 15.6 ± standard deviation of 8.0 months. Two patients had already been intubated at a previous hospital because they presented with severe respiratory failure and required emergency intubation. One patient was intubated upon arrival to our hospital. We identified three reasons for the delay in diagnosis: delayed referral to a neurologist (four patients); a shortage of neurologists in rural areas (three patients); and an atypical clinical course with respiratory failure as the initial symptom (two patients). Three patients had undergone emergency intubation without giving informed consent. To provide an informed choice and to avoid unwanted intubation for ALS patients, we suggest extending neurological knowledge of ALS to general practitioners.

1. Introduction

Amyotrophic lateral sclerosis (ALS) is a progressive, neurodegenerative disorder that causes muscle weakness, disability, respiratory failure, and eventually death. The annual incidence of ALS is one to three cases per 100,000 people worldwide. ALS commonly strikes people from 40 to 60 years old, and men are affected slightly more often than women. Most ALS patients in Japan are diagnosed by neurologists using the El Escorial criteria [1].

In this report, we review the clinical characteristics of seven ALS patients who were not correctly diagnosed until their admission to our hospital. We have studied the reasons for the delayed diagnosis of ALS.

2. Patients and methods

We retrospectively reviewed all 200 patients diagnosed with sporadic ALS who met the criteria for either definite or probable ALS [1] in our hospital from January 2001 to April 2011. Among them, we focused on seven patients who had shown ALS symptoms, but were not correctly diagnosed by general physicians. These patients were finally diagnosed with ALS when they developed severe respiratory failure and were admitted to our hospital. We reviewed their age, sex, residential district, symptoms of onset, diagnosis before admission, time between onset and admission, medical institutions attended, type of ALS, ALS Functional Rating Scale-Revised, Norris scale [2,3], arterial blood gases, respiratory function, and outcome. To describe the regional differences between the areas where the patients lived, we reviewed the population and medical resources in the secondary medical districts defined by the Japanese government [4].

The initial symptoms of ALS were classified as limb-type (upper or lower limb weakness), progressive bulbar palsy-type (bulbar palsy), or respiratory onset-type (respiratory failure).

Results are presented as mean ± standard deviation.

3. Results

3.1. Background and clinical course

The clinical characteristics of our seven patients are shown in Table 1. They accounted for 3.5% of all ALS patients admitted over

* Corresponding author. Tel.: +81 86 235 7365; fax: +81 86 235 7368.
E-mail address: kosatou@cc.okayama-u.ac.jp (K. Abe).

http://dx.doi.org/10.1016/j.jocn.2013.11.021
0967-5868/

10 years. Their mean age at admission was 68.1 ± 5.6 years, and the male to female ratio was 1:2.

Although all the patients had developed respiratory failure by the time of their admission to our hospital, only two patients showed dyspnea as an initial symptom. Five of the seven patients (71.4%) were diagnosed with weight loss of unknown cause at the first hospital they attended, and the mean time from onset to a correct diagnosis (Ta) was 15.6 ± 8.0 months. However, the mean Ta of Patients 1, 2, 3, 5, and 6 was 19.8 months (much longer than that of the other two patients, for whom the mean Ta was 5 months). Four patients were seen in a clinic or hospital for over 10 months (Patients 1, 2, 5, 6), before admission to our hospital, without a diagnosis of ALS. During this period, the mean number of medical institutions they visited or were admitted to was 1.3 ± 0.8, and the mean time that they spent in other institution(s) was 8.7 ± 7.6 months (approximately half of the 15.6 months from onset to diagnosis). They were tentatively diagnosed with weight loss, depression, myasthenia gravis, cancer, cervical spondylosis, pneumonia, or Sjögren syndrome.

As for the ALS types, four patients were limb-type, two were respiratory onset-type, and one was progressive bulbar palsy-type. The mean ALS Functional Rating Scale-Revised score, Norris limb, and Norris bulbar scale scores were 18.1 ± 11.9, 19.3 ± 15.9, and 21.9 ± 13.1, respectively. The mean arterial blood gas results when respiratory failure became apparent were pH 7.34 ± 0.09, pO_2 68.6 ± 11.8 mmHg, and pCO_2 70.0 ± 22.5 mmHg. Respiratory function could be measured in three patients, and the mean percentage forced vital capacity was 27 ± 12.8%. However, two patients (Patients 1, 5; Table 1) had already been intubated at a previous hospital because they presented with severe respiratory failure and required emergency intubation. Eventually, two patients died of respiratory failure, three patients were transferred to other hospitals after tracheotomy and endotracheal intubation, and the other two were discharged (one patient with endotracheal intubation and the other with non-invasive positive pressure ventilation [NNPV]).

3.2. Geographical analysis

Our hospital is located in the southeast district of the Okayama prefecture in western Japan. The Okayama prefecture faces the Kagawa prefecture over the Seto Inland Sea. These two prefectures are closely related economically and socially, because they are connected by a long bridge over the inland sea. Most of the patients who visit our hospital are from the Okayama prefecture, but some patients are from the Kagawa prefecture. Okayama prefecture is

Table 1
Clinical characteristics of the seven amyotrophic lateral sclerosis (ALS) patients

Patient	1	2	3	4	5	6	7
Admission year	2006	2007	2009	2010	2010	2010	2011
Age of onset, years	70	68	64	60	68	69	78
Sex	F	F	F	M	M	F	F
Resident district	Northeast district in Okayama	Southeast district in Okayama	Northeast district in Okayama	Southeast district in Okayama	Central district in Kagawa	Southeast district in Okayama	Northeast district in Okayama
Population (population density, per sq. km)	198,000 (107.3)	907,000 (477.6)	198,000 (107.3)	907,000 (477.6)	455,000 (978.1)	907,000 (477.6)	198,000 (107.3)
Medical doctors (per 100,000 people)	340 (171.5)	2758 (303.4)	340 (171.5)	2758 (303.4)	1291 (283.8)	2758 (303.4)	340 (171.5)
Neurology specialists (per 100,000 people)	5 (2.5)	45 (5.0)	5 (2.5)	45 (5.0)	14 (3.1)	45 (5.0)	5 (2.5)
Symptoms of onset	Neck weakness	Lower limb weakness	Hand grip weakness	Exertional dyspnea	Exertional dyspnea	Dysarthria	Sholder girdle weakness
Diagnosis before admission	Weight loss	Weight loss Depression Cervical spondylosis	Weight loss Depression	Myasthenia gravis	Esophageal cancer Pneumonia	Weight loss Dysphasia due to Sjorgren syndrome	Weight loss Cervical spondylosis
Time from onset to first medical contact, months	1	2	20	–	4	3	3
Medical institutions and time until admission (doctor's specialty)	• Clinic (physician) for 18 months	• Hospital (orthopedist) for 12 months • Clinic (physician) for 4 months	• Hospital (physician) for 1 month • Hospital (psychologist) for 3 months	–	• Hospital (surgeon) for 11 months	• Hospital (brain surgeon) for 16 months • Hospital (physician) for 3 months	• Hospital (orthopedist) for 3 months
Time between onset to admission, months	18	18	24	4	15	24	6
Type of ALS	Limb	Limb	Limb	Respiratory onset	Respiratory onset	PBP	Limb
ALSFRS-R	7	18	15	31	3	36	17
Norris Limb	17	14	8	31	7	50	8
Norris Bulbar	13	25	14	48	9	26	18
Arterial blood gas	pH 7.18 pO_2 85.9 mmHg pCO_2 106.6 mmHg	pH 7.41 pO_2 73.4 mmHg pCO_2 59.8 mmHg	pH 7.30 pO_2 63.1 mmHg pCO_2 78.0 mmHg	pH 7.41 pO_2 70.8 mmHg pCO_2 52.3 mmHg	pH 7.29 pO_2 47.2 mmHg pCO_2 85.7 mmHg	pH 7.40 pO_2 71.5 mmHg pCO_2 66.3 mmHg	pH 7.41 pO_2 68.1 mmHg pCO_2 39.0 mmHg
% FVC	Unmeasurable (mechanical ventilation)	0.2	0.16	0.45	Unmeasurable (mechanical ventilation)	0.26	Unmeasurable (critical condition)
Outcome	Transferred to other hospital	Discharged to home	Death	Transferred to other hospital	Transferred to other hospital	Discharged to home	Death

ALSFRS-R = Amyotrophic Lateral Sclerosis Functional Rating Scale-Revised, F = female, FVC = forced vital capacity, M = male, PBP = progressive bulbar palsy, sq. = square.

divided into five secondary medical districts by the Japanese government; the same is the case for the Kagawa prefecture. Our seven patients were from three districts of these two prefectures: three from the northeast district of Okayama prefecture (Patients 1, 3, 7), three from the southeast district of Okayama prefecture (Patients 2, 4, 6), and one from the central district of Kagawa prefecture (Patient 5; Table 1). In the northeast district of Okayama, there are fewer medical doctors per head of population (171.5 per 100,000 people) than the Japanese average (223.9 per 100,000 people). Moreover, in the northeast district of Okayama and the central district of Kagawa, there are fewer neurology specialists (2.5 and 3.1 per 100,000 people, respectively) than the Japanese average (3.7 per 100,000 people). The population density of the northeast district of Okayama is one third of the Japanese average (107.3 and 338.8 per km^2, respectively).

4. Discussion

The focus of this study was to determine the reason that these seven patients were not diagnosed with ALS until they presented with respiratory failure. The diagnostic delay from onset to diagnosis of ALS varies from case to case, but many retrospective studies have reported a mean delay of 8.0–15.6 months [5–14]. Factors that affect the diagnostic delay have been noted as spinal onset [9,14], patient age of 65–75 years, fasciculation as first symptom [9], incorrect use of heuristics [14], and delay in referral to a neurologist [6,14].

In this study, the mean Ta was 15.6 months; this is at the top end of the previously reported range. We suggest three reasons for this. Firstly, the diagnosis of ALS was not considered by the doctors for a long time (Patients 1, 2, 5, 6). These patients might have initially presented with muscle weakness and atrophy, indicating the lower motor neuron dysfunction characteristic of ALS, but they were not referred to a neurologist at this early stage. A previous report showed that the period from first medical contact to first neurology visit accounted for 45% of the time from onset to diagnosis. However, for these four patients, this accounted for 86.7% of the time to diagnosis.

Secondly, three patients (Patients 1, 3, 7) lived in a rural northeast district, which has a low population density (one third of the Japanese average) and fewer neurologists (two thirds of the Japanese average). We assume that there is a shortage of neurologists in other such districts, despite an adequate number of medical doctors.

Thirdly, two patients (Patients 4, 5) presented with atypical symptoms in the early stages of ALS. Respiratory failure in ALS generally follows weakness of the limbs or bulbar palsy, but these patients presented initially with respiratory dysfunction. In such cases, diagnosis of ALS would be difficult. Although these are rare cases, Shoesmith et al. reported that 2.7% of ALS patients demonstrate respiratory failure as the initial symptom [15].

Impaired respiratory function is a negative prognostic factor in ALS [16,17]. However, several studies have shown that NPPV improves the prognosis of individuals with ALS [18,19]. In addition, attempting NPPV treatment may improve the prognosis of ALS with respiratory onset [15]. Among our patients, four first received endotracheal intubation, another received NPPV, and the other two declined mechanical ventilation. Three patients who were admitted to our hospital had been intubated without advanced informed consent, but two patients were subsequently discharged.

To reduce the time from onset to diagnosis, and to avoid unwanted intubation and tracheotomy for ALS patients, we should extend our neurological knowledge to general practitioners in the local community, especially in rural areas where there is a shortage of such specialists. Although ALS is a rare disease, similar situations to those described here may occur in other countries.

Conflicts of Interest/Disclosures

The authors declare that they have no financial or other conflicts of interest in relation to this research and its publication.

References

[1] Brooks BR, Miller RG, Swash M, et al. El Escorial revisited: revised criteria for the diagnosis of amyotrophic lateral sclerosis. Amyotroph Lateral Scler Other Motor Neuron Disord 2000;1:293–9.
[2] Oda E, Ohashi Y, Tashiro K, et al. Reliability and factorial structure of a rating scale for amyotrophic lateral sclerosis. No To Shinkei 1996;48:999–1007.
[3] Ohashi Y, Tashiro K, Itoyama Y, et al. Study of functional rating scale for amyotrophic lateral sclerosis: revised ALSFRS(ALSFRS-R) Japanese version. No To Shinkei 2001;53:346–55.
[4] Minister's Secretariat Ministry of Health, Labour and Welfare. White papers & reports: Annual health, labour and welfare, Report 2008–2009. Tokyo; Ministry of Health, Labour and Welfare; 2009.
[5] Pongratz D. The diagnostic process in ALS. J Neurol Sci 1999;165:S10–3.
[6] Househam E, Swash M. Diagnostic delay in amyotrophic lateral sclerosis: what scope for improvement? J Neurol Sci 2000;180:76–81.
[7] Traynor BJ, Codd MB, Corr B, et al. Clinical features of amyotrophic lateral sclerosis according to the El Escorial and Airlie house diagnostic criteria: a population-based study. Arch Neurol 2000;57:1171–6.
[8] Czaplinski A, Yen AA, Simpson EP, et al. Slower disease progression and prolonged survival in contemporary patients with amyotrophic lateral sclerosis: is the natural history of amyotrophic lateral sclerosis changing? Arch Neurol 2006;63:1139–43.
[9] Zoccolella S, Beghi E, Palagano G, et al. Predictors of delay in the diagnosis and clinical trial entry of amyotrophic lateral sclerosis patients: a population-based study. J Neurol Sci 2006;250:45–9.
[10] Donaghy C, Dick A, Hardiman O, et al. Timeliness of diagnosis in motor neurone disease: a population-based study. Ulster Med J 2008;77:18–21.
[11] Chio A, Mora G, Calvo A, et al. Epidemiology of ALS in Italy: a 10-year prospective population-based study. Neurology 2009;72:725–31.
[12] Kraemer M, Buerger M, Berlit P. Diagnostic problems and delay of diagnosis in amyotrophic lateral sclerosis. Clin Neurol Neurosurg 2010;112:103–5.
[13] Okita T, Nodera H, Shibuta Y, et al. Can Awaji ALS criteria provide earlier diagnosis than the revised El Escorial criteria? J Neurol Sci 2011;302:29–32.
[14] Cellura E, Spataro R, Taiello AC, et al. Factors affecting the diagnostic delay in amyotrophic lateral sclerosis. Clin Neurol Neurosurg 2012;114:550–4.
[15] Shoesmith CL, Findlater K, Rowe A, et al. Prognosis of amyotrophic lateral sclerosis with respiratory onset. J Neurol Neurosurg Psychiatry 2007;78:629–31.
[16] Czaplinski A, Yen AA, Appel SH. Forced vital capacity (FVC) as an indicator of survival and disease progression in an ALS clinic population. J Neurol Neurosurg Psychiatry 2006;77:390–2.
[17] Stambler N, Charatan M, Cedarbaum JM. Prognostic indicators of survival in ALS. ALS CNTF Treatment Study Group. Neurology 1998;50:66–72.
[18] Aboussouan LS, Khan SU, Meeker DP, et al. Effect of noninvasive positive-pressure ventilation on survival in amyotrophic lateral sclerosis. Ann Intern Med 1997;127:450–3.
[19] Kleopa KA, Sherman M, Neal B, et al. Bipap improves survival and rate of pulmonary function decline in patients with ALS. J Neurol Sci 1999;164:82–8.

Neurobiology of Disease 69 (2014) 200–205

Contents lists available at ScienceDirect

Neurobiology of Disease

journal homepage: www.elsevier.com/locate/ynbdi

LDB3 splicing abnormalities are specific to skeletal muscles of patients with myotonic dystrophy type 1 and alter its PKC binding affinity

Yoshihiro Yamashita [a,1], Tohru Matsuura [a,b,*,1], Tatsuaki Kurosaki [a], Yoshinobu Amakusa [a], Masanobu Kinoshita [c], Tohru Ibi [d], Ko Sahashi [d], Kinji Ohno [a]

[a] Division of Neurogenetics, Center for Neurological Diseases and Cancer, Nagoya University Graduate School of Medicine, Nagoya, Japan
[b] Division of Neurology, Department of Medicine, Jichi Medical University, Shimotsuke, Japan
[c] Department of Frontier Health Sciences, Graduate School of Human Health Sciences, Tokyo Metropolitan University, Tokyo, Japan
[d] Department of Neurology, Aichi Medical University School of Medicine, Aichi, Japan

ARTICLE INFO

Article history:
Received 24 January 2014
Revised 6 May 2014
Accepted 19 May 2014
Available online 27 May 20147

Keywords:
Myotonic dystrophy type 1
Muscleblind-like 1
CUG triplet repeat RNA-binding protein
LIM domain binding 3
Protein kinase C

ABSTRACT

Myotonic dystrophy type 1 (DM1) is caused by transcription of CUG repeat RNA, which causes sequestration of muscleblind-like 1 (MBNL1) and upregulation of CUG triplet repeat RNA-binding protein (CUG-BP1). In DM1, dysregulation of these proteins contributes to many aberrant splicing events, causing various symptoms of the disorder. Here, we demonstrate the occurrence of aberrant splicing of LIM domain binding 3 (*LDB3*) exon 11 in DM1 skeletal muscle. Exon array surveys, RT-PCR, and western blotting studies demonstrated that exon 11 inclusion was DM1 specific and could be reproduced by transfection of a minigene containing the CTG repeat expansion. Moreover, we found that the *LDB3* exon 11-positive isoform had reduced affinity for PKC compared to the exon 11-negative isoform. Since PKC exhibits hyperactivation in DM1 and stabilizes CUG-BP1 by phosphorylation, aberrant splicing of *LDB3* may contribute to CUG-BP1 upregulation through changes in its affinity for PKC.

Introduction

Myotonic dystrophy (DM) is the most common cause of adult-onset muscular dystrophy. The symptoms of DM are systemic, affecting multiple organs, such as the skeletal muscle (myotonia, muscle wasting), heart (arrythmia, conduction defects, dilated cardiomyopathy), brain (dementia, sleeplessness), and endocrine system (insulin resistance) (Harper, 2001). The most common form of the disease is DM type 1 (DM1), an autosomal dominant inherited disorder caused by a CTG repeat expansion in the 3′-untransrated region (UTR) of the *DMPK* gene. The etiology of DM1 is mainly the gain of function achieved by a toxic mRNA (Osborne and Thornton, 2006; Ranum and Cooper, 2006). RNA containing expanded CUG repeats sequesters an important splicing factor, muscleblind-like 1 (MBNL1). On the other hand, another splicing factor, CUG triplet repeat RNA-binding protein (CUG-BP1), is overexpressed in conjunction with expression of the toxic repeat-containing RNA. Dysregulation of these 2 splicing factors is thought to cause aberrant splicing events in various genes and results in systemic symptoms observed in patients with DM1 (Osborne and Thornton, 2006; Ranum and Cooper, 2006).

To date, 28 aberrantly spliced exons have been identified in striated muscle. Additionally, exon array analysis of aberrant splicing events identified 2 previously described DM1-specific events (Yamashita et al., 2012). Among these events, aberrantly spliced LIM domain binding 3 (*LDB3*) is known to play an integral role in the interaction between the muscular Z-line and α-actinin-2 (Faulkner et al., 1999; Zhou et al., 1999). Moreover, mutations or depletions in *LDB3* are associated with dilated cardiomyopathy and myofibrillar myopathy (Arimura et al., 2004, 2009; Cheng et al., 2011; Griggs et al., 2007; Vatta et al., 2003; Xing et al., 2006; Zheng et al., 2009; Zhou et al., 2001), which are closely related to the cardiac symptoms of DM.

LDB3 interacts with protein kinase C (PKC) through its C-terminal LIM domains (Zhou et al., 1999). In DM1, PKC is inappropriately activated and phosphorylates CUG-BP1, leading to its overexpression (Kuyumcu-Martinez et al., 2007). Therefore, we speculated that aberrant splicing of *LDB3* may change the affinity of the LDB3 protein for PKC and contribute to variations in PKC activation. In the current study, we investigated the specificity of aberrant splicing of *LDB3* exon 11 to DM1 skeletal muscle and the effects of inclusion of exon 11 on the affinity of the LDB3 long isoform for PKC.

* Corresponding author at: Division of Neurology, Department of Medicine, Jichi Medical University, 3311-1 Yakushiji, Shimotsuke, Tochigi 329-0498, Japan. Fax: +81 285 44 5118.
E-mail address: tohrum@jichi.ac.jp (T. Matsuura).**Available online on ScienceDirect (www.sciencedirect.com).**
[1] These authors contributed equally to this work.

http://dx.doi.org/10.1016/j.nbd.2014.05.026
0969-9961/

Materials and methods

Patient samples

DM1 skeletal muscles were previously biopsied for diagnostic purposes ($n = 8$, at Aichi Medical University, details given in Table 1). All the samples were diagnosed with Southern blot analysis to confirm the approximate repeat numbers. Three normal control muscle specimens showing no pathological abnormalities were used. Disease controls were also previously biopsied for diagnostic purposes, including samples from patients with amyotrophic lateral sclerosis (ALS), spinal and bulbar muscular atrophy (SBMA), Becker type muscular dystrophy (BMD), Duchenne type muscular dystrophy (DMD), and polymyositis/dermatomyositis (PM/DM). Detailed information about the biopsy samples is given in Table 1. High-molecular-weight DNA was extracted by the conventional proteinase K and phenol chloroform method. We determined the CTG repeat numbers at the 3′ UTR of the *DMPK* gene by Southern blotting (Table 1). Statistical analysis of differences between the samples was performed by Student's *t*-test.

All experiments were approved by the Institutional Review Board of Nagoya University Graduate School of Medicine and Aichi Medical University. The samples were used for the current studies after appropriate informed consent was obtained from all patients.

Skeletal muscle RT-PCR

We searched for aberrant splicing in DM1 skeletal muscle using a GeneChip Human *Exon* 1.0 ST Array according to our previously described methods (Yamashita et al., 2012). Total RNA was extracted with the RNeasy Mini Kit (Qiagen, Valencia, CA, USA), according to the manufacturer's protocol. We reverse transcribed 100 ng of total RNA using SuperScript II (Invitrogen, Carlsbad, CA, USA) with oligo $(dT)_{15}$ primers. Then, we performed PCR using the cDNA as a template, 2X Master Mix (Qiagen), and 0.2 μM flanking primers on exon 8 and exon 12 (FWD: 5′-GGACCTTGCCGTAGACA, REV: GTAGACAGAAGGCCGGAT). The Multiplex RT-PCR was performed using Multiplex PCR Kit (Qiagen). Primers were as follows. For long isoform (FWD on exon 16: 5′-GTCCCA TTCCCATCTCCAC, REV on exon 17: GCCCTCACTGTAGCTGGTGT); short isoform (FWD on exon 9: 5′-CGAAGGTCAAGGGAAAGGTT, REV on exon 10: TTAACATTAAGGATTTGGGCTGA). We used 3 primers as follows for separating each LDB3 isoform: exon 3 (FWD: 5′-GTCCCATTCCCATCTC CAC), exon 10 (REV: AAACGTGGGCTGTTACGTTC), exon 12 (REV: GGTA GACAGAAGGCCGGATG). Electrophoresis was performed using ethidium bromide-stained 2.5% agarose gels.

LDB3 exon 11 minigene assay

First, we constructed the *LDB3* exon 11 minigene, which consisted of fragments containing an end region of exon 9 (34 bp, full length 37 bp) and downstream intron of exon 9 (1552 bp), an upstream intron of exon 11 (1357 bp) and exon 11 (189 bp), downstream intron of exon 11 (3185 bp, full length), and a part of exon 12 (73 bp, full length 146 bp; Fig. 1A). Each fragment was PCR-amplified using human genomic DNA as a template with KOD -plus- (Toyobo, Tokyo, Japan). Then, each fragment was ligated into pcDNA3.1 (Invitrogen) using the *NheI*/*NotI*/*XhoI* site. Constructing a minigene containing the full length intron around exon 11 was difficult since the length of the upstream intron was too long (13,959 bp). One microgram of the minigene was cotransfected into C2C12 cells (60% confluent) in 6-well plates with DMPK, DT960, GFP-CUGBP1, or GFP-MBNL1 40 kDa using Lipofectamine 2000 (Invitrogen). Cells were harvested, and total RNA was extracted with the RNeasy Mini Kit (Qiagen). RT-PCR was performed using a forward primer targeting the pcDNA3.1 site (FWD: AGAAGCTCTGCGAAGGTC AA) and a reverse primer targeting *LDB3* exon 12 (REV: CAACAGATGG CTGGCAACTA).

Table 1
Skeletal muscle samples used for RT-PCR and western blotting.

Samples	Age/sex	Biopsy site	# of DM1 expanded repeat
DM1 1[a]	58/F	IBi	1450 (WBC[b])
DM1 2[a]	40/M	IBi	4500 (muscle)
DM1 3[a]	38/F	IBi	4230 (muscle)
DM1 4	30/F	IBi	4000 (muscle)
DM1 5	52/F	IBi	3430 (muscle)
DM1 6	44/M	IB	4300 (muscle)
DM1 7	22/F	rVL	3830 (muscle)
DM1 8	47/M	IBi	3770 (muscle)
ALS 1	58/M	rVL	
ALS 2	45/F	lVL	
SBMA 1	55/M	IBi	
BMD 1	27/M	IB	
BMD 2	35/M	IBi	
DMD 1	1/M	lVL	
DMD 2	7/M	IBi	
PM/DM 1	51/F	rVL	
PM/DM 2	52/F	rVL	
FSH 1	19/M	IBi	
FSH 2	41/M	IBi	
IBM 1	75/M	lQ	
IBM 2	68/F	rTA	
NC 1	51/F	lVL	
NC 2[a]	77/M	unknown	
NC 3[a]	71/F	unknown	

DM1: myotonic dystrophy type 1; ALS: amyotrophic lateral sclerosis; SBMA: spinal bulbar muscular atrophy; BMD: Becker type muscular dystrophy; DMD: Duchenne type muscular dystrophy; PM/DM: polymyositis/dermatomyositis; FSH: facioscapulohumeral muscular dystrophy; IBM: inclusion body myositis; NC: normal control.
IBi: left biceps; rVL, lVL: right or left vastus lateralis; lQ: left quadriceps; rTA: right tibias anterior.
[a] Only RNA but not protein samples were available.
[b] White blood cells.

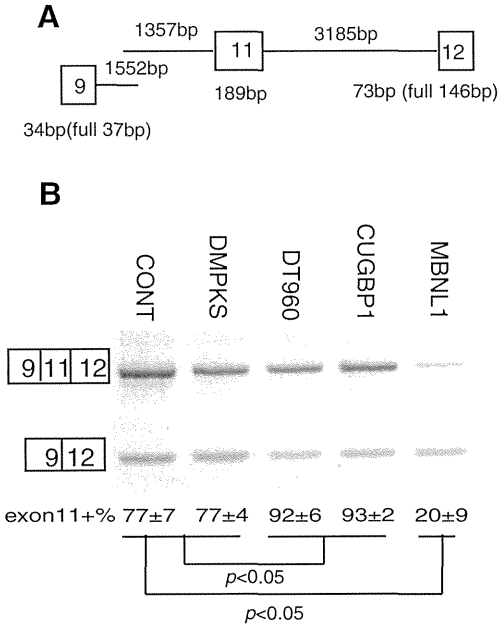

Fig. 1. CTG repeat expansion caused exon 11 inclusion. A. Schematic representation of the LDB3 exon11 minigene containing 34 bp of exon 9, 1552 bp downstream of exon 9, 1357 bp upstream of exon 11, exon 11 (189 bp), 3185 bp downstream of exon 11, and 73 bp of exon 12. B. RT-PCR of the LDB3 exon 11 minigene transfection assay. Average rates of exon 11-containing PCR products are shown at the bottom of the figure, and ± indicates the SE (standard error, $n = 3$). Lanes represent minigenes transfected with minigene only, DMPKS (the DMPK construct with no repeat expansion), DT960 (the DMPK construct with the 960 CTG repeat expansion), CUGBP1, and MBNL1.

Western blotting of skeletal muscle protein

Proteins were extracted from human skeletal muscle biopsies. Tissues were homogenized with a polytron in lysis buffer (50 mM Tris–HCl, pH 7.5, 0.15 M NaCl, 1 mM EDTA, 1% NP-40, and 1 protease inhibitor cocktail tablet). Homogenates were centrifuged (20 min, 12,000 rpm), and the pellet was discarded. Protein concentrations were determined by the Bradford assay (Bio-Rad, Hercules, CA, USA). Additional samples were added to confirm splice isoform specificity to DM1. Total proteins extracts (50 μg) were separated on 12% SDS-PAGE gels and transferred onto nitrocellulose membranes. The membranes were blocked with 5% nonfat dry milk in TBS-T buffer (Tris buffer saline plus 0.1% Tween-20). Incubation with primary antibodies (anti-LDB3 antibodies, ab40840, Abcam) was performed overnight at 4 °C at a concentration 3:50,000 in TBS-T buffer, followed by incubation for 1 h with secondary antibodies (1:5000, ExactaCruz, Santa Cruz Biotechnology, Santa Cruz, CA, USA) in 1% skim milk.

LDB3 and PKC isoform construction

The LDB3 long isoform (exon 11-negative or exon 11-positive) and short isoform were LA-PCR amplified from human cDNA and inserted into the *p3xFLAG*-CMV-7.1 vector (Sigma Aldrich, St. Louis, MO, USA) at the *BglII*-*KpnI* restriction site. PKCα, PKCβ, and PKCε were also LA-PCR amplified from commercial templates and inserted into myc-tagged vectors (gift from Kozo Kaibuchi, Nagoya University Graduate School of Medicine).

Immunoprecipitation assay

Two micrograms of FLAG-tagged LDB3 short isoform, long exon 11-negative isoform, or long exon 11-positive isoform was cotransfected with 2 μg of myc-tagged PKCα, PKCβ, or PKCε into COS-7 cells. Twenty-four hours later, proteins were extracted with lysis buffer (as above) and centrifuged (20 min, 12,000 rpm). Immunoprecipitation was performed using anti-myc-Tag agarose (mouse IgG1, MBL), according to the manufacturer's protocol. Cell lysates and immunoprecipitated products were separated on 10% SDS-PAGE gels, transferred to membranes, and incubated with primary antibodies (anti-myc 9E10, 1:2000, Abcam; anti-FLAG M2, 1:5000, Sigma). ECL-anti-mouse IgG (1:5000, GE Healthcare) was used as the secondary antibody. The binding affinity of FLAG-tagged LDB3 isoforms for myc-tagged PKCs was calculated by dividing the intensity of anti-FLAG with the intensity of anti-myc in western blotting of immunoprecipitated products.

Results

Aberrant splicing of exon 11 was specific to DM1

LDB3 was identified as having an aberrantly spliced exon by our previous exon array studies (Yamashita et al., 2012). Exon 4 and exon 11 (previously termed as exon 7 by us) were both included specifically in DM1. In this paper, exon 11 is identical to exon 7 in our previous report, in which the exon number was based on NM_007078.2 in the NCBI RefSeq database. Exon 11 is the 11th exon when all exons in all the transcripts annotated by ENSEMBL release 68 are taken into account. The LDB3 isoform containing exon 11 was observed in more than 50% of mRNA in DM1 samples, but less than 20% in control samples and samples from other diseases. Differences between the DM1 and normal control groups and between the DM1 and disease control groups were statistically significant ($p < 0.05$).

Aberrant splicing was caused by expansion of CTG repeats

To assess which factors contributed to abnormal splicing of *LDB3* exon 11, we performed overexpression assays by cotransfecting C2C12 cells with an *LDB3* exon 11 minigene and other constructs. DT960 (containing 960 CTG repeats and expressing 960 CUG without protein expression) promoted exon 11 inclusion compared to DMPK (including no repeat, Fig. 1). Therefore, we assumed that CTG repeat expansion itself was a contributing factor for exon 11 inclusion. In addition, CUG-BP1 overexpression promoted exon 11 inclusion, while MBNL1 overexpression decreased exon 11 inclusion.

An isoform shift was also observed at the protein level

Although aberrant splicing of *LDB3* exon 11 was confirmed at the mRNA level, its effect on protein expression was not clear. Alternative splicing of exons 5, 6, and 11 as well as alternative transcription termination predicts six LDB3 isoforms (Fig. 2A). All isoforms are either registered in the RefSeq database or in a previous report (Faulkner et al., 1999). Western blot analyses using skeletal muscle biopsy samples and antibodies targeting LDB3 revealed that the exon 11-positive isoform was expressed at significantly higher levels in DM1 muscles than in control muscles and muscle samples from patients with other neuromuscular disorders (Fig. 2B). These results demonstrated that DM1 samples clearly contained more of the exon 11-positive LDB3 isoform than samples from other disorders. Western blot analysis also revealed that more long isoform (78 kDa and 84 kDa) was expressed than short isoform (32 kDa) in DM1 (Fig. 2B). The difference was statistically significant ($p < 0.05$). We then analyzed the expression of the short and long isoforms with multiplex RT-PCR (Fig. 2C). The long isoform was also predominant in DM1 with statistical significance ($p < 0.05$).

To discriminate cardiac and skeletal isoforms, we performed multiplex RT-PCR with 3 primers with the forward primer on exon 3, the reverse primer on exon 10 (the final exon of short isoform), and on exon 12 (Fig. 2D). The exon 5-6-8-9-11-positive product was predominant in DM1. Importantly, the exon 4 positive isoform seemed to be not mainly expressed in DM1. We generated *LDB3* clones using DM1 cDNA as a template. Among 10 long isoform clones, no exon 4-positive ones were found (data not shown).

We found the exon 5-6-negative-7 (6a)-positive isoform (bottom band) only in DM1 samples as previously reported (Fig. 2D).

Aberrant splicing changed PKC-binding affinity

Because LDB3 has been shown to bind to PKC, we next investigated differences in the binding affinities of various LDB3 isoforms for PKC (Figs. 2A and 3). Importantly, the amounts of FLAG-tagged LDB3 isoforms and myc-tagged PKC isoforms expressed following transfection were similar, and myc-tagged PKC isoforms were immunoprecipitated with similar efficiencies. We observed that exon 11-positive LDB3 exhibited about 50% reduced binding affinity for PKCα and PKCβ compared to exon 11-negative LDB3. No significant difference was observed in terms of PKCε binding affinities between exon 11-negative and -positive LDB3 (Fig. 3, bottom panels).

Discussion

The importance of LDB3 and the specificity of aberrant exon 11 splicing to DM1

In DM1, many structural proteins in muscle fibers are aberrantly spliced, including α-dystrobrevin (Nakamori et al., 2008), BIN1 (Fugier et al., 2011), CAPN3 (Lin et al, 2006), DMD (Nakamori et al., 2007), DTNA, LDB3 (Lin et al., 2006; Yamashita et al., 2012), MYOM1 (Koebis et al., 2011), MYH14 (Rinaldi et al., 2012), NRAP (Lin et al., 2006), PDLIM3 (ALP) (Ohsawa et al., 2011), TNNT2, TNNT3 (Philips et al., 1998), and TTN (Lin et al., 2006; Yamashita et al., 2012). Among these, aberrant splicing of *BIN1* exon 11 has been shown to be associated with T tubule alterations and muscle weakness *in vivo* and *in vitro*.

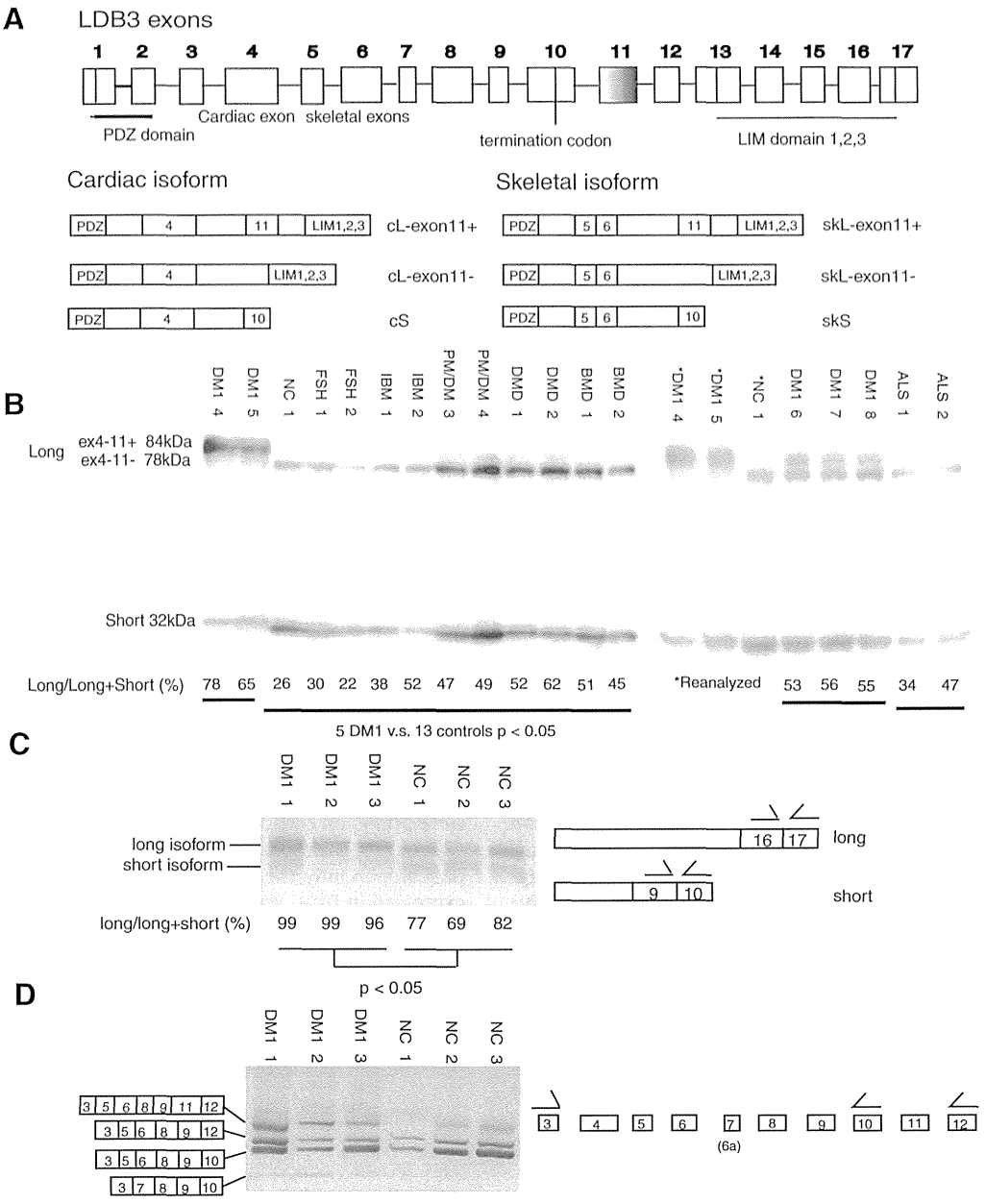

Fig. 2. Exon 11 splicing abnormalities were present at the protein level and specific to DM1. *LDB3* long isoforms were predominantly expressed in DM1, and exon 4 was rarely expressed. A. Schematic diagram of LDB3 isoforms. Cardiac isofoms included exon 4, whereas skeletal isoforms included exons 5 and 6. cL-exon11 +: cardiac long isoform with exon 11, cL-exon11-: cardiac long isoform without exon11, cS: cardiac short isoform, skL-exon11 +: skeletal muscle long isoform with exon 11, skL-exon11-: skeletal muscle long isoform without exon 11, skS: skeletal muscle short isoform. B. Western blotting of skeletal muscles using anti-LDB3 antibodies. The upper band for DM1 was 84 kDa containing exon 11 and the lower band was around 78 kDa, without exon 11. The short isoform was 35 kDa ($n = 5$ DM1 samples). The difference of long/(long + short) ratio was statistically significant between DM1 and other samples ($p < 0.05$). C. Multiplex RT-PCR to detect long and short isoform. The difference between DM1 and normal control was statistically significant ($p < 0.05$). D. Multiplex RT-PCR to detect exon expression from exon 3 to exon 12. Exon 5 and 6-positive isoforms were predominantly expressed in DM1.

However, the roles of aberrant splicing of other muscular structural proteins in the pathogenesis of DM1 remain to be elucidated.

In this study, we focused on the aberrant splicing of LDB3 because 1) LDB3 exists in Z-lines, key sections of muscle fibers required for contraction (Faulkner et al., 1999; Zhou et al., 1999); 2) LDB3 interacts with PKC (Zhou et al., 1999), which is upregulated in DM1 and stabilizes CUG-BP1 (Kuyumcu-Martinez et al., 2007); and 3) mutations or depletion of LDB3 result in cardiac symptoms similar to those observed in patients with DM1 (Arimura et al., 2004, 2009; Bhakta et al., 2004; Cheng et al., 2011; Griggs et al., 2007; Groh et al., 2008; Vatta et al., 2003; Xing et al., 2006; Zheng et al., 2009; Zhou et al., 2001). Our study demonstrated that abnormal inclusion of *LDB3* exon 11 was specific to DM1. Indeed, although the inclusion of *LDB3* exon 11 in DM1 has been reported previously (Lin et al., 2006; Vihola et al., 2010), the specificity of this missplicing event to DM1 had not been fully assessed.

Inclusion of LDB3 exon 4 in DM1 skeletal muscles

LDB3 is known to have long (over 70 kDa) and short (about 32 kDa) isoforms (Huang et al., 2003). Although the long isoform observed in DM1 was reported to contain not only exon 11 but also exon 4, which is specific to cardiac tissue (Lin et al., 2006; Vihola et al., 2010), our efforts to sequence 10 clones following the amplification of *LDB3* cDNA from DM1 skeletal muscles demonstrated that all clones including exon 11 did not contain exon 4, but did contain exons 5 and 6, which are specific to skeletal muscle. RT-PCR also revealed that exon 4

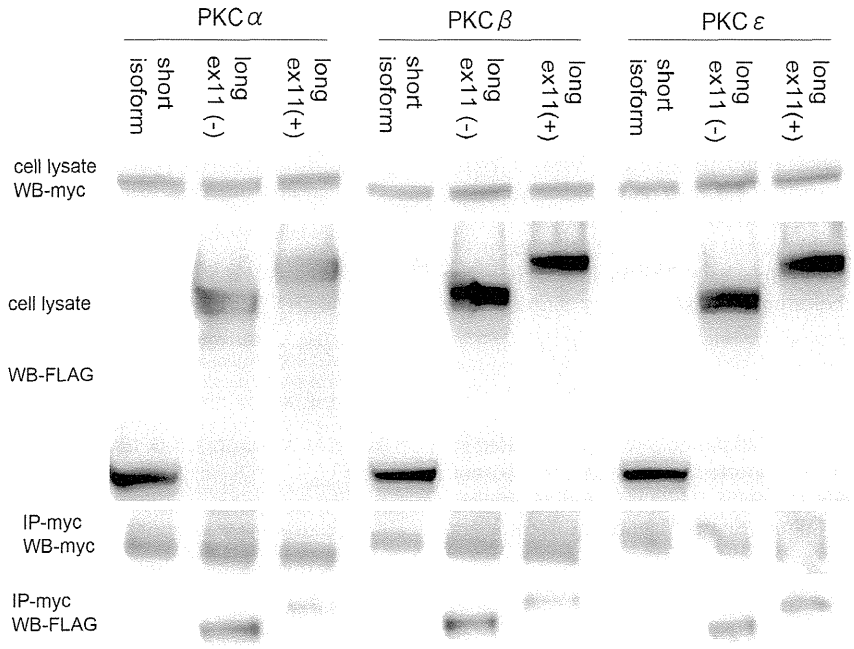

Fig. 3. The LDB3 exon 11 + isoform exhibited reduced binding affinity to PKCα and PKCβ. Cotransfections with LDB3 isoforms and PKC isoforms were performed, and whole cell lysates were harvested. Immunoprecipitation was then performed using these whole cell lysates. The ratio of FLAG/myc was calculated in order to quantify the binding affinity of FLAG-tagged LDB3 isoforms with myc-tagged PKCs.

expression was not predominant in DM1 (Fig. 2D). This suggested that the uppermost band (84 kDa) observed in western blotting represented the exon 11-positive long isoform, while the 78-kDa band represented the exon 11-negative long isoform, and the 32-kDa band represented the exon 11-negative short isoform, consistent with data presented in previous literature (Vihola et al., 2010). In any case, our data clarified that the abnormal exon 11-positive long isoform was overexpressed in DM1 skeletal muscles.

In a previous study, we reported that exon 4 inclusion was specific to DM1 muscles (Yamashita et al., 2012). Although this is somewhat contradictory to the current study, it is possible that the exon 4-positive long isoform (i.e., the cardiac exon) may be very rare compared to the isoform containing exons 5 and 6 (skeletal exons). On the other hand, inclusion of *LDB3* exon 4 may also contribute to the pathogenesis of DM1. Interestingly, mutations in *LDB3* exon 4 have been shown to reduce the affinity of LDB3 for PGM1 and are associated with dilated cardiomyopathy (Arimura et al., 2009). Thus, inclusion of exon 4 in LDB3 from DM1 skeletal muscles may change the affinity of LDB3 for PGM1 and lead to muscular structural changes and weakness.

Exon 7 inclusion and skipping of exons 5 and 6

We also confirmed exon 7(6a) inclusion and skipping of exon 5 and 6 in DM1 (Fig. 2D) as previously described (Machuca-Tzili et al., 2006). The pathogenic role of this mis-splicing also remains to be elucidated.

Factors influencing the regulation of exon 11 splicing

In this study, we confirmed that CTG repeats caused *LDB3* exon 11 inclusion. Moreover, overexpression of MBNL1 led to exclusion of exon 11, while overexpression of CUG-BP1 led to inclusion of exon 11. Thus, although another report suggested that MBNL1 is the only factor regulating the splicing of *LDB3* exon 11 (Kalsotra et al., 2008), CUG-BP1 may also be involved in the regulation of exon 11 splicing (Fig. 1). The antagonistic effect of MBNL1 overexpression was more prominent than that of CTG repeat or CUG-BP1 overexpression. This may be due to the basal high inclusion (about 70%) of exon 11 minigene, and the existence of 11 candidate MBNL1 YGCY binding sites (Goers et al., 2010) (7 and 4 in the bilateral flanking 500 bp upstream and downstream introns, respectively, from SpliceAid: http://www.introni.it/splicing.html).

LDB3 isoforms and PKC binding affinity

We next considered the functional significance of *LDB3* exon 11 inclusion in the pathogenesis of DM1. The long isoform of *LDB3* interacts with PKC through its LIM domain, while the short isoform does not. Although exon 11 is not a part of LIM domain, its existence may alter the binding affinity of the LDB3 long isoform to PKCs since it is located near the LIM domain. Our current data demonstrated that the exon 11-positive isoform had only about 50% of the affinity for PKCα and PKCβ compared to the exon 11-negative isoform, while no significant difference was observed in terms of PKCε affinity.

In DM1, PKCs are hyperactivated by unknown mechanisms, leading to stabilization of CUG-BP1 (Kuyumcu-Martinez et al., 2007; Wang et al., 2009). Consistent with this, CUG-BP1 is upregulated in DM1 and is thought to contribute to various phenotypes observed in patients with DM1 (Koshelev et al., 2010; Wang et al., 2009). The importance of PKC activity in DM1 pathogenesis is clear. Thus, LDB3 may function as an anchoring protein to stabilize PKCs to the Z-line and subsequently suppress PKC activation. However, in DM1, the exon 11-positive isoform of LDB3 may have reduced ability to anchor PKC enzymes, thereby promoting hyperactivation of PKCα and PKCβ. Interestingly, PKC activation is achieved rapidly (within 6 h) after administration of CTG repeat RNA (Kuyumcu-Martinez et al., 2007). Thus, hyperactivation of PKC enzymes may be induced through another mechanism.

The LDB3 long isoform also has important functions as a cytoskeletal muscle protein. Mutations in LDB3 have been shown to be associated with dilated cardiomyopathy and left ventricular noncompaction (Arimura et al., 2004, 2009; Cheng et al., 2011; Griggs et al., 2007; Vatta et al., 2003; Xing et al., 2006; Zheng et al., 2009; Zhou et al., 2001). In particular, mutations in the LIM domain of the long isoform have been shown to alter the binding affinity of LDB3 for PKCα, PKCβ, and PKCε (Arimura et al., 2004).

The long isoform has also been suggested to have more important functions than the short isoform. For example, in mice, depletion of a selective cypher (human LDB3) long, not short, isoform has been shown to

lead to late-onset cardiomyopathy (Cheng et al., 2011). In this study, we proved that the long isoforms are predominant ones in DM1 (Fig. 2B and C). Although this difference was statistically significant, the effect might be driven by a small amount of long isoform in FSH and a large amount of long isoform in DM1 (4 and 5). The long isoforms may play an important role in DM1 patients compared to other diseases. Thus, since point mutations in LDB3 have been shown to cause cardiomyopathy, exon inclusion likely has a major impact on muscular phenotype.

In summary, we identified abnormal inclusion of *LDB3* exon 11 specific to DM1 at the RNA and protein level. This inclusion changed the affinity of LDB3 for PKC, indicating that exon 11 may contribute to the activation of PKC in DM1.

Acknowledgments

We appreciate the cooperation of all patients who participated in this investigation. This study was supported by JSPS KAKENHI (Grant Numbers: 20200078, 21390266, 23659455, 24390083, and 24390221) from the Ministry of Education, Culture, Sports, Science and Technology of Japan.

References

Arimura, T., Hayashi, T., Terada, H., Lee, S.-Y., Zhou, Q., Takahashi, M., et al., 2004. A Cypher/ZASP mutation associated with dilated cardiomyopathy alters the binding affinity to protein kinase C. J. Biol. Chem. 279, 6746–6752.

Arimura, T., Inagaki, N., Hayashi, T., Shichi, D., Sato, A., Hinohara, K., et al., 2009. Impaired binding of ZASP/Cypher with phosphoglucomutase 1 is associated with dilated cardiomyopathy. Cardiovasc. Res. 83, 80–88.

Bhakta, D., Lowe, M.R., Groh, W.J., 2004. Prevalence of structural cardiac abnormalities in patients with myotonic dystrophy type I. Am. Heart J. 147, 224–227.

Cheng, H., Zheng, M., Peter, A.K., Kimura, K., Li, X., Ouyang, K., et al., 2011. Selective deletion of long but not short Cypher isoforms leads to late-onset dilated cardiomyopathy. Hum. Mol. Genet. 20, 1751–1762.

Faulkner, G., Pallavicini, A., Formentin, E., Comelli, A., Ievolella, C., Trevisan, S., et al., 1999. ZASP: a new Z-band alternatively spliced PDZ-motif protein. J. Cell Biol. 146, 465–475.

Fugier, C., Klein, A.F., Hammer, C., Vassilopoulos, S., Ivarsson, Y., Toussaint, A., et al., 2011. Misregulated alternative splicing of BIN1 is associated with T tubule alterations and muscle weakness in myotonic dystrophy. Nat. Med. 17, 720–725.

Goers, E.S., Purcell, J., Voelker, R.B., Gates, D.P., Berglund, J.A., 2010. MBNL1 binds GC motifs embedded in pyrimidines to regulate alternative splicing. Nucleic Acids Res. 38, 2467–2484.

Griggs, R., Vihola, A., Hackman, P., Talvinen, K., Haravuori, H., Faulkner, G., et al., 2007. Zaspopathy in a large classic late-onset distal myopathy family. Brain 130, 1477–1484.

Groh, W.J., Groh, M.R., Saha, C., Kincaid, J.C., Simmons, Z., Ciafaloni, E., et al., 2008. Electrocardiographic abnormalities and sudden death in myotonic dystrophy type 1. N. Engl. J. Med. 358, 2688–2697.

Harper, P.S., 2001. Myotonic dystrophy, 3rd ed. W. B. Saunders,.

Huang, C., Zhou, Q., Liang, P., Hollander, M.S., Sheikh, F., Li, X., et al., 2003. Characterization and in vivo functional analysis of splice variants of cypher. J. Biol. Chem. 278, 7360–7365.

Kalsotra, A., Xiao, X., Ward, A., Castle, J., Johnson, J., Burge, C.B., et al., 2008. A postnatal switch of CELF and MBNL proteins reprograms alternative splicing in the developing heart. Proc. Natl. Acad. Sci. U. S. A. 105, 20333–20338.

Koebis, M., Ohsawa, N., Kino, Y., Sasagawa, N., Nishino, I., Ishiura, S., 2011. Alternative splicing of myomesin 1 gene is aberrantly regulated in myotonic dystrophy type 1. Genes Cells 16, 961–972.

Koshelev, M., Sarma, S., Price, R.E., Wehrens, X.H.T., Cooper, T.A., 2010. Heart-specific overexpression of CUGBP1 reproduces functional and molecular abnormalities of myotonic dystrophy type 1. Hum. Mol. Genet. 19, 1066–1075.

Kuyumcu-Martinez, N.M., Wang, G.-S., Cooper, T.A., 2007. Increased steady-state levels of CUGBP1 in myotonic dystrophy 1 are due to PKC-mediated hyperphosphorylation. Mol. Cell 28, 68–78.

Lin, X., Miller, J.W., Mankodi, A., Kanadia, R.N., Yuan, Y., Moxley, R.T., et al., 2006. Failure of MBNL1-dependent post-natal splicing transitions in myotonic dystrophy. Hum. Mol. Genet. 15, 2087–2097.

Machuca-Tzili, L., Thorpe, H., Robinson, T.E., Sewry, C., Brook, J.D., 2006. Flies deficient in Muscleblind protein model features of myotonic dystrophy with altered splice forms of Z-band associated transcripts. Hum. Genet. 120 (4), 487–499.

Nakamori, M., Kimura, T., Fujimura, H., Takahashi, M.P., Sakoda, S., 2007. Altered mRNA splicing of dystrophin in type 1 myotonic dystrophy. Muscle Nerve 36, 251–257.

Nakamori, M., Kimura, T., Kubota, T., Matsumura, T., Sumi, H., Fujimura, H., et al., 2008. Aberrantly spliced alpha-dystrobrevin alters alpha-syntrophin binding in myotonic dystrophy type 1. Neurology 70, 677–685.

Ohsawa, N., Koebis, M., Suo, S., Nishino, I., Ishiura, S., 2011. Alternative splicing of PDLIM3/ALP, for α-actinin-associated LIM protein 3, is aberrant in persons with myotonic dystrophy. Biochem. Biophys. Res. Commun. 409, 64–69.

Osborne, R.J., Thornton, C.A., 2006. RNA-dominant diseases. Hum. Mol. Genet. 15, R162–R169.

Philips, A.V., Timchenko, L.T., Cooper, T.A., 1998. Disruption of splicing regulated by a CUG-binding protein in myotonic dystrophy. Science 280, 737–741.

Ranum, L.P., Cooper, T.A., 2006. RNA-mediated neuromuscular disorders. Annu. Rev. Neurosci. 29, 259–277.

Rinaldi, F., Terracciano, C., Pisani, V., Massa, R., Loro, E., Vergani, L., et al., 2012. Aberrant splicing and expression of the non muscle myosin heavy-chain gene MYH14 in DM1 muscle tissues. Neurobiol. Dis. 45, 264–271.

Vatta, M., Mohapatra, B., Jimenez, S., Sanchez, X., Faulkner, G., Perles, Z., et al., 2003. Mutations in Cypher/ZASP in patients with dilated cardiomyopathy and left ventricular non-compaction. J. Am. Coll. Cardiol. 42, 2014–2027.

Vihola, A., Bachinski, L.L., Sirito, M., Olufemi, S.-E., Hajibashi, S., Baggerly, K.A., et al., 2010. Differences in aberrant expression and splicing of sarcomeric proteins in the myotonic dystrophies DM1 and DM2. Acta Neuropathol. 119, 465–479.

Wang, G.S., Kuyumcu-Martinez, M.N., Sarma, S., Mathur, N., Wehrens, X., Cooper, T.A., 2009. PKC inhibition ameliorates the cardiac phenotype in a mouse model of myotonic dystrophy type 1. J. Clin. Invest. 119, 3797–3806.

Xing, Y., Ichida, F., Matsuoka, T., Isobe, T., Ikemoto, Y., Higaki, T., et al., 2006. Genetic analysis in patients with left ventricular noncompaction and evidence for genetic heterogeneity. Mol. Genet. Metab. 88, 71–77.

Yamashita, Y., Matsuura, T., Shinmi, J., Amakusa, Y., Masuda, A., Ito, M., et al., 2012. Four parameters increase the sensitivity and specificity of the exon array analysis and disclose 25 novel aberrantly spliced exons in myotonic dystrophy. J. Hum. Genet. 57, 368–374.

Zheng, M., Cheng, H., Li, X., Zhang, J., Cui, L., Ouyang, K., et al., 2009. Cardiac-specific ablation of Cypher leads to a severe form of dilated cardiomyopathy with premature death. Hum. Mol. Genet. 18, 701–713.

Zhou, Q., Ruiz-Lozano, P., Martone, M.E., Chen, J., 1999. Cypher, a striated muscle-restricted PDZ and LIM domain-containing protein, binds to alpha-actinin-2 and protein kinase C. J. Biol. Chem. 274, 19807–19813.

Zhou, Q., Chu, P.H., Huang, C., Cheng, C.F., Martone, M.E., Knoll, G., et al., 2001. Ablation of Cypher, a PDZ-LIM domain Z-line protein, causes a severe form of congenital myopathy. J. Cell Biol. 155, 605–612.

RESEARCH ARTICLE

Inactivation of PNKP by Mutant ATXN3 Triggers Apoptosis by Activating the DNA Damage-Response Pathway in SCA3

Rui Gao[1], Yongping Liu[1¤], Anabela Silva-Fernandes[2,3], Xiang Fang[1], Adriana Paulucci-Holthauzen[4], Arpita Chatterjee[5], Hang L. Zhang[1], Tohru Matsuura[6], Sanjeev Choudhary[5], Tetsuo Ashizawa[7], Arnulf H. Koeppen[8], Patricia Maciel[2,3], Tapas K. Hazra[5], Partha S. Sarkar[1,9]*

1 Department of Neurology, University of Texas Medical Branch, Galveston, Texas, United States of America, **2** Life and Health Sciences Research Institute (ICVS), School of Health Sciences, University of Minho, Braga, Portugal, **3** ICVS/3B's PT Government Associate Laboratory, Braga/Guimarães, Portugal, **4** Department of Biomedical Engineering, University of Texas Medical Branch, Galveston, Texas, United States of America, **5** Department of Internal Medicine, University of Texas Medical Branch, Galveston, Texas, United States of America, **6** Department of Neurology, Jichi Medical School, Shimotsuke, Japan, **7** Department of Neurology and McNight Brain Research Institute, University of Florida, Gainesville, Florida, United States of America, **8** Department of Neurology, Albany Stratton VA Medical Center, Albany, New York, United States of America, **9** Neuroscience and Cell Biology, University of Texas Medical Branch, Galveston, Texas, United States of America

¤ Current address: Department of Physiology, Xiangya School of Medicine, Central South University, Changsha, Hunan, PR China
* pssarkar@utmb.edu

Citation: Gao R, Liu Y, Silva-Fernandes A, Fang X, Paulucci-Holthauzen A, Chatterjee A, et al. (2015) Inactivation of PNKP by Mutant ATXN3 Triggers Apoptosis by Activating the DNA Damage-Response Pathway in SCA3. PLoS Genet 11(1): e1004834. doi:10.1371/journal.pgen.1004834

Editor: Christopher E. Pearson, The Hospital for Sick Children and University of Toronto, CANADA

Received: March 14, 2014

Accepted: October 16, 2014

Published: January 15, 2015

Data Availability Statement: All relevant data are within the paper and its Supporting Information files.

Funding: This study was funded by NIH grant NS073976 to TKH and a John Sealy Grant to PSS. The funders had no role in study design, data collection and analysis, decision to publish, or preparation of the manuscript.

Competing Interests: The authors have declared that no competing interests exist.

Abstract

Spinocerebellar ataxia type 3 (SCA3), also known as Machado-Joseph disease (MJD), is an untreatable autosomal dominant neurodegenerative disease, and the most common such inherited ataxia worldwide. The mutation in SCA3 is the expansion of a polymorphic CAG tri-nucleotide repeat sequence in the C-terminal coding region of the *ATXN3* gene at chromosomal locus 14q32.1. The mutant ATXN3 protein encoding expanded glutamine (polyQ) sequences interacts with multiple proteins *in vivo*, and is deposited as aggregates in the SCA3 brain. A large body of literature suggests that the loss of function of the native ATNX3-interacting proteins that are deposited in the polyQ aggregates contributes to cellular toxicity, systemic neurodegeneration and the pathogenic mechanism in SCA3. Nonetheless, a significant understanding of the disease etiology of SCA3, the molecular mechanism by which the polyQ expansions in the mutant ATXN3 induce neurodegeneration in SCA3 has remained elusive. In the present study, we show that the essential DNA strand break repair enzyme PNKP (polynucleotide kinase 3'-phosphatase) interacts with, and is inactivated by, the mutant ATXN3, resulting in inefficient DNA repair, persistent accumulation of DNA damage/strand breaks, and subsequent chronic activation of the DNA damage-response ataxia telangiectasia-mutated (ATM) signaling pathway in SCA3. We report that persistent accumulation of DNA damage/strand breaks and chronic activation of the serine/threonine kinase ATM and the downstream p53 and protein kinase C-δ pro-apoptotic pathways trigger neuronal dysfunction and eventually neuronal death in SCA3. Either PNKP overexpression

or pharmacological inhibition of ATM dramatically blocked mutant ATXN3-mediated cell death. Discovery of the mechanism by which mutant ATXN3 induces DNA damage and amplifies the pro-death signaling pathways provides a molecular basis for neurodegeneration due to PNKP inactivation in SCA3, and for the first time offers a possible approach to treatment.

Author Summary

Spinocerebellar ataxia type 3 (SCA3) is an untreatable neurodegenerative disease, and the most common dominantly inherited ataxia worldwide. SCA3 is caused by expansion of a CAG tri-nucleotide repeat sequence in the *ATXN3* gene's coding region. The expanded CAG sequences encode a run of the amino acid glutamine; the mutant ATXN3 interacts with multiple proteins *in vivo* to create insoluble aggregates in SCA3 brains. It is thought that the loss of function of the aggregated proteins contributes to cellular toxicity and neurodegeneration in SCA3. Despite significant progress in understanding SCA3's etiology, the molecular mechanism by which the mutant protein triggers the death of neurons in SCA3 brains remains unknown. We now report that the mutant ATXN3 protein interacts with and inactivates PNKP (polynucleotide kinase 3'-phosphatase), an essential DNA strand break repair enzyme. This inactivation results in persistent accumulation of DNA damage, and chronic activation of the DNA damage-response ATM signaling pathway in SCA3. Our work suggests that persistent DNA damage/strand breaks and chronic activation of ATM trigger neuronal death in SCA3. Discovery of the mechanism by which mutant ATXN3 induces DNA damage and amplifies the pro-death pathways provides a molecular basis for neurodegeneration in SCA3, and perhaps ultimately for its treatment.

Introduction

Spinocerebellar ataxia type 3 (SCA3), also known as Machado-Joseph disease (MJD), is an autosomal dominant neurodegenerative disease caused by CAG repeat expansion in the C-terminal coding region of the *ATXN3* gene [1–3]. SCA3 is the most common dominantly inherited ataxia world-wide, and a late-onset disease that manifests with cerebellar ataxia, peripheral nerve palsy, and pyramidal and extrapyramidal signs [1–4]. SCA3 neurodegeneration is primarily observed in the brainstem, cerebellum, basal ganglia and spinal cord [5–8]. Ataxia symptoms appear between the ages of 20 and 50 years, and manifest with cerebellar ataxia, opthalmoplegia, dysarthria, dysphagia, dystonia, rigidity and distal muscle atrophies [1–3, 8, 9]. The wild-type *ATXN3* gene encodes 12 to 41 CAG repeats in its 10^{th} exon at the human chromosomal locus 14q32.1 [3]. ATXN3 is a deubiquitinating enzyme that edits specific poly-ubiquitin linkages [10, 11]. It has also been linked to transcriptional regulation [9, 12]. However, ATXN3 does not seem to be essential for brain development and function, as mice lacking ATXN3 do not develop overt neurological phenotypes [13]. Therefore, the exact function of ATXN3 remains unknown, limiting efforts to establish the possible role of mutant ATXN3 in eliciting neuronal death in SCA3. In SCA3, the polymorphic CAG repeats are expanded to 62 to 84 glutamines and the mutant ATXN3 forms aggregates that are deposited in SCA3 neurons [2, 3]. A large body of literature supports the hypothesis that multiple proteins aberrantly interact with the mutant ATXN3 and that the loss of function of the mutant ATXN3-interacting proteins contributes to neurodegeneration and SCA3 pathology [2, 8–9]. Recent studies have reported that

depletion of the mutant ATXN3 allele in a SCA3 transgenic mouse brains rescues the molecular phenotypes of SCA3 supporting the hypothesis that mutant ATXN3 elicits toxicity and neuronal dysfunction in SCA3 [14]. Recent studies have also shown that the mutant ATXN3 causes p53-mediated neuronal death *in vitro* and *in vivo* by activating the transcription of the p53-inducibe pro-apoptotic genes such as *BAX* (Bcl2-associated X protein) and *PMAIP1* (PUMA, p53 upregulated modulator of apoptosis), triggering mitochondrial apoptotic pathways [15, 16]. However, the mechanism by which mutant ATXN3 increases p53 phosphorylation and activates the p53-dependent pro-apoptotic signaling pathways to facilitate neuronal death and dysfunction remains unknown.

In the present study we show that PNKP (Polynucleotide kinase 3'-phosphatase), a dual-function DNA strand break repair enzyme [17, 18], is a native ATXN3-interacting protein, and is inactivated by its interaction with the mutant ATXN3 in SCA3. Our data also show that PNKP is also present, in part in the polyQ aggregates in SCA3 brain. Diminished PNKP activity results in persistent accumulation of DNA strand breaks, leading to chronic activation of the DNA damage-response ataxia telangiectasia mutated (ATM) protein kinase and the downstream pro-apoptotic p53-dependent signaling pathways in SCA3. Additionally, activated ATM stimulates phosphorylation of c-Abl tyrosine kinase, which phosphorylates and facilitates nuclear inclusion of protein kinase C delta (PKCδ), further amplifying pro-apoptotic output in SCA3. Either overexpression of PNKP or pharmacological inhibition of ATM in mutant ATXN3-expressing cells blocked aberrant activation of the pro-death pathways and reduced cell death, suggesting that mutant ATXN3-mediated chronic activation of the DNA damage-response ATM signaling pathway plays a pivotal role in neuronal dysfunction and neurodegeneration in SCA3. Therefore, our current study not only provides an insight into the mechanism of neurodegeneration in SCA3, but also delineates potential drug targets for developing mechanism-based efficacious therapeutic modalities to combat systemic degeneration of neuronal cells in SCA3.

Results

PNKP interacts with the mutant ATXN3 and is sequestered into the ATXN3-polyQ aggregates in SCA3 brain

Our studies described in the accompanying manuscript by Chatterjee et al suggest that PNKP is a native ATXN3-interacting protein, and that ATXN3 modulates PNKP activity and DNA repair (Chatterjee et al, Figs. 1–3). Immunoprecipitation of PNKP from the nuclear extract from human neuroblastoma SH-SY5Y cells and subsequent mass spectrometric analysis showed the presence of ATXN3 in the immunoprecipitated (IP) pellet; conversely, immunoprecipitation of ATXN3 and Western blot analysis revealed the presence of PNKP in the ATXN3 IP (Chatterjee et al, Figs. 1, S1, 2A and 2B). Further, GST pull-down from the nuclear extract, followed by Western blot analysis, indicated that both wild-type and mutant ATXN3 directly interact with PNKP *in vitro*, (Chatterjee et al; Fig. 2D). The wild-type ATXN3 protein stimulated, and in contrast, the mutant ATXN3 dramatically diminished, the 3' phosphatase activity of PNKP *in vitro* (Chatterjee et al; Figs. 3A and 3B). The interaction between these two proteins was further validated in SH-SY5Y cells co-transfected with the plasmids pCherry-PNKP and pGFPC-ATXN3–28, expressing cherry-tagged PNKP and GFP-tagged ATXN3-Q28, respectively, and imaged by confocal microscopy. Analysis of the transfected cells showed significant co-localization of the red fluorescence of PNKP with the green fluorescence of ATXN3-Q28 (Fig. 1A). Similarly, cells co-transfected with pCherry-PNKP and pGFP-ATXN3-Q84 (a plasmid expressing mutant ATXN3-Q84 encoding 84 glutamines) showed marked co-localization of PNKP and ATXN3-Q84 (Fig. 1B). However, co-transfection of plasmid

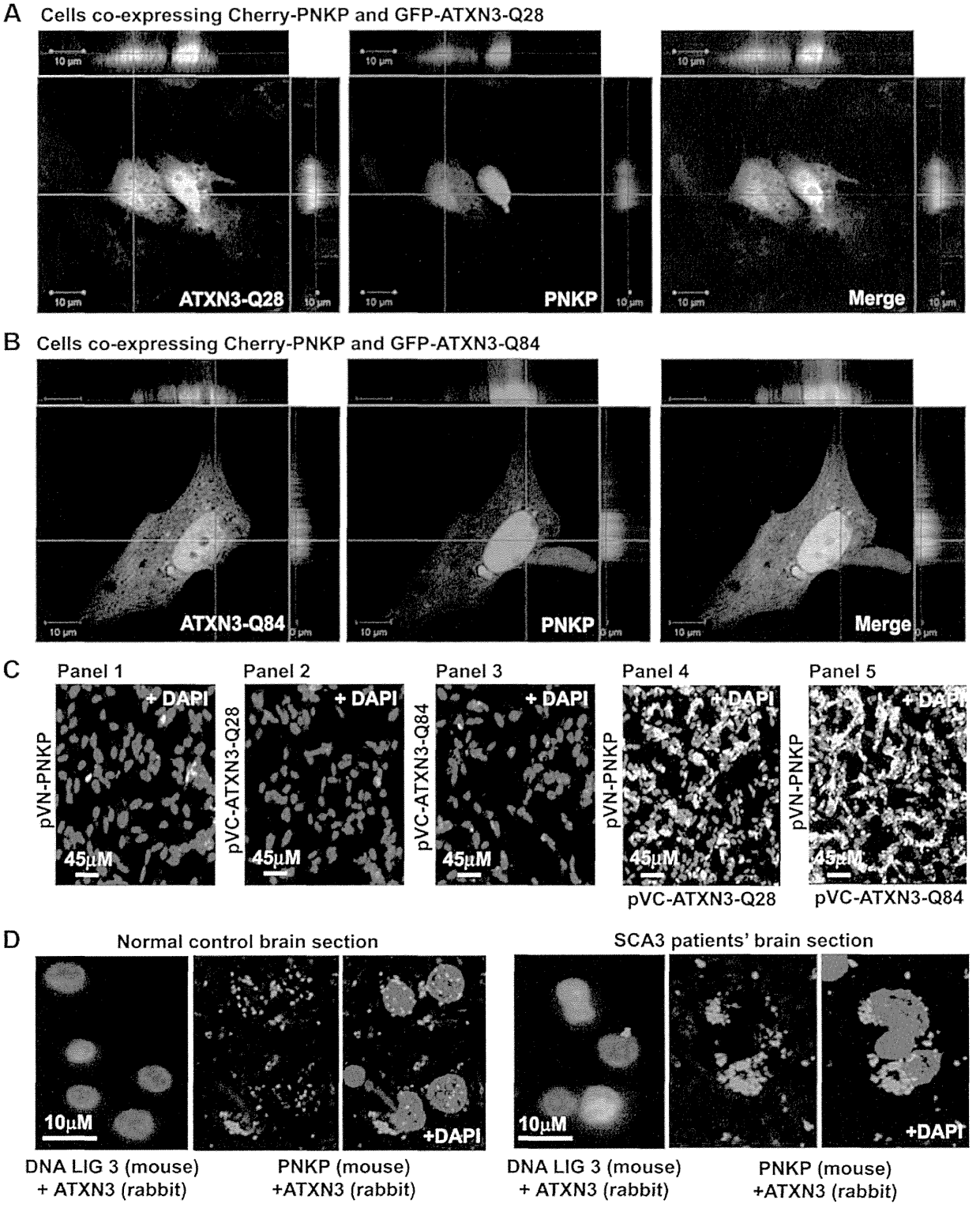

Figure 1. PNKP interacts with both wild-type and mutant ATXN3 in cells and human brain sections. (A) Plasmids pGFP-ATXN3-Q28 and pCherry-PNKP were co-transfected into SH-SY5Y cells and co-localization of PNKP and ATXN3-Q28 was assessed by confocal microscopy; the merge of green and red fluorescence from ATXN2-Q28 and PNKP, respectively, appears as yellow/orange fluorescence. Nuclei were stained with DAPI in C-D. **(B)** Plasmids pGFP-ATXN3-Q84 and pCherry-PNKP were co-transfected into SH-SY5Y cells and co-localization of PNKP and ATXN3-Q84 was assessed as in A.

(C) Bimolecular fluorescence complementation assay. SH-SY5Y cells were transfected with plasmid: Panel 1) pVN173-PNKP; Panel 2) pVC155-ATXN3-Q28; Panel 3) pVC155-ATXN3-Q84; Panel 4) co-transfected with pVN173-PNKP and pVC155-ATXN3-Q28; or Panel 5) pVN173-PNKP and pVC155-ATXN3-Q84. Reconstitution of green/yellow fluorescence was assessed 48 hours after transfection using fluorescence microscopy (20X). Nuclei were stained with DAPI in Figs. 1C and 1D. **(D)** Proximity ligation assays (PLAs) were performed on control and SCA3 human brain sections, using mouse anti-PNKP and rabbit anti-ATXN3 primary antibodies, and anti-DNA ligase 3 (DNA LIG3) (rabbit) with anti-ATXN3 (mouse) antibodies as control. The generation of red fluorescence was monitored under a fluorescence microscope.

doi:10.1371/journal.pgen.1004834.g001

pCherry-PNKP and pAcGFPC1 (an empty control vector expressing GFP) did not show any detectable reconstitution of yellow/orange fluorescence (S1 Fig.), suggesting specificity of these interactions. Together, these data support our previous interpretation that both wild-type and mutant ATXN3 interact with PNKP in the cell (Chatterjee et al).

To further confirm the interaction of PNKP and ATXN3 *in cell*, we performed bi-molecular fluorescence complementation (Bi-FC) assays, a versatile method to assess *in cell* protein-protein interactions [19]. We cloned PNKP cDNA with the N-terminal amino acids of modified GFP into plasmid pBiFC-VN173, and ATXN3 cDNA (encoding 28 and 84 glutamines) with the C-terminal amino acids of modified GFP into plasmid pBiFC-VC155 (a description of these Bi-FC plasmids is provided in the Methods section). Transfection of pVN173-PNKP, pVC155-ATXN3-Q28 or pVC155-ATXN3-Q84 into SH-SY5Y cells individually did not reconstitute green/yellow fluorescence (Fig. 1C, panels 1–3). In contrast, co-transfection of plasmids pVN173-PNKP and pVC155-ATXN3-Q28 effectively reconstituted green/yellow fluorescence (Fig. 1C, panel 4). Importantly, co-transfection of plasmids pVN173-PNKP and pVC155-ATXN3-Q84 also resulted in robust reconstitution of green/yellow fluorescence (Fig. 1C, panel 5). These data substantiate our interpretation that both wild-type and mutant ATXN3 interact with PNKP in the cell. Furthermore, we analyzed these protein-protein interactions in SCA3 patients' brain sections by proximity ligation assays (PLA), a widely used technique to assess *in vivo* protein-protein interactions [20]. The PLA analysis clearly shows a robust reconstitution of red fluorescence in both SCA3 and normal control brains, suggesting an *in vivo* interaction between ATXN3 and PNKP (n = 3; Fig. 1D). Importantly, about 70% of the ATXN3-PNKP complexes were detected in the nuclei in the control brain sections (Fig. 1D; panel 2 and 3). By contrast, PLA analysis of the SCA3 patients' brain sections shows that the ATXN3-PNKP complexes are predominantly present in periphery or outside the nuclei (n = 3, Fig. 1D). Since PNKP is present in the mitochondria [18], the extra-nuclear signals detected in the control brain sections presumably are from the PNKP-ATXN3 complexes present in the mitochondria. To further verify the specificity of the *in vivo* interaction of ATXN3 and PNKP, we performed PLA analysis to check the interaction of ATXN3 with DNA ligase 3α (DNA LIG 3α), another critical DNA strand break repair enzyme present in the PNKP complex (Chatterjee et al; Figs. 2A, 2B and S2). The PLA analysis showed no significant interaction of ATXN3 with DNA LIG 3α in the brain sections from SCA3 patients, or in control brains under identical experimental conditions (Fig. 1D; panels 1 and 4), suggesting specificity of the interactions between ATXN3 and PNKP *in vivo*. Consistent with these data, PLA analysis also suggested specific and pronounced interactions of ATXN3 and PNKP in SH-SY5Y cells (accompanying manuscript, Chatterjee et al, Fig. 2C).

The *in vivo* interaction of PNKP and ATXN3 in SCA3 and control brain sections was further confirmed by immunostaining brain sections from SCA3 patients and control subjects with specific antibodies, followed by confocal microscopy. For immunostaining the brain sections we used an anti-PNKP antibody that shows high specificity for PNKP as evidenced by Western blot and immunohistochemical analyses (S2 Fig.). Image analysis revealed a distinct co-localization of PNKP with ATXN3 in the cerebellum of normal control brain and SCA3 (expressing mutant ATXN3 with 72 glutamines, ATXN3-Q72) brain sections (Figs. 2A and 2B).

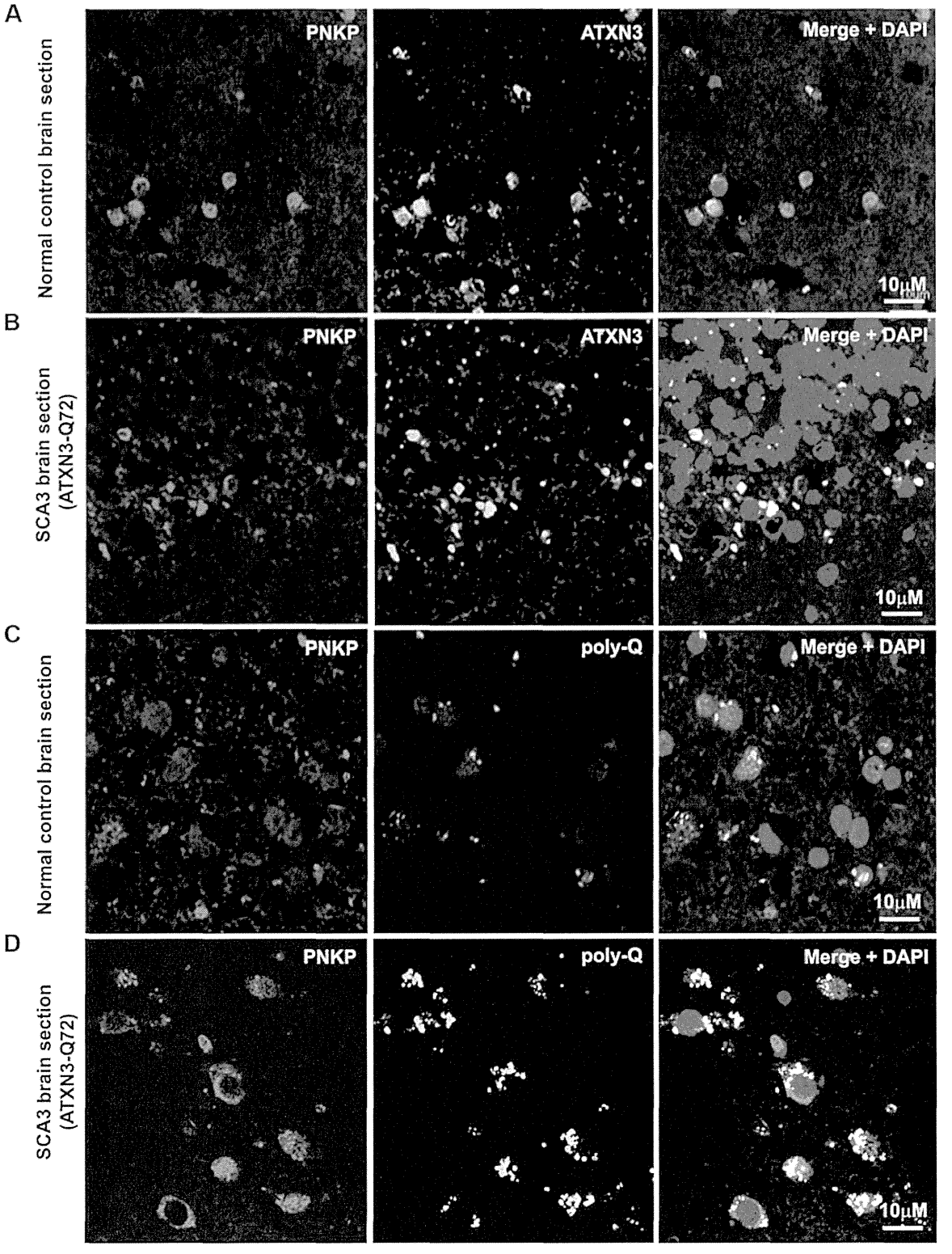

Figure 2. PNKP co-localizes with wild-type and mutant ATXN3 in human brain sections. (A) Normal human brain sections were analyzed by immunostaining with anti-PNKP (red) and anti-ATXN3 (green) antibodies to assess *in vivo* interaction of PNKP and ATXN3; merge of red and green fluorescence appears as yellow/orange fluorescence, Nuclei were stained with DAPI in Figs. 1A to 1D; **(B)** SCA3 (expressing mutant ATXN3-Q72) brain sections were analyzed by immunostaining with anti-PNKP (red), and anti-ATXN3 (green) antibodies to assess *in vivo* interaction of PNKP and ATXN3;